energy&fuels

pubs.acs.org/EF

Article

Asphaltene Precipitation and Deposition during Nitrogen Gas Cyclic Miscible and Immiscible Injection in Eagle Ford Shale and Its Impact on Oil Recovery

Mukhtar Elturki and Abdulmohsin Imqam*

Cite This: *Energy Fuels* 2022, 36, 12677−12694

Read Online

ACCESS | Metrics & More | Article Recommendations | Supporting Information

ABSTRACT: Cyclic gas injection methods have been shown to improve oil recovery in conventional reservoirs. Even though similar technologies have been used in unconventional reservoirs with some success stories in shale resources, cyclic gas injection enhanced oil recovery (EOR) is still a little-understood subject in boosting oil recovery from unconventional reservoirs. During gas injection, asphaltenes start to deposit and precipitate, which causes pore plugging and reduces oil recovery. Studies of asphaltene deposition challenges during cyclic nitrogen (N_2) gas injection and oil production in unconventional reservoirs are yet relatively limited. Therefore, a comprehensive experimental study was conducted using 12 Eagle Ford shale cores (dynamic mode), and filter paper membranes (static mode) were used to evaluate whether miscible and immiscible huff-n-puff (cyclic) N_2 injection increases oil recovery and aggravates asphaltene precipitation. To ensure that miscibility can be examined in cyclic experiments, N_2 minimum miscibility pressure (MMP) was determined using a slim tube technique. The factors studied included the injection pressure, number of cycles, production time, and injection cyclic mode, all conducted at 70 °C. The findings showed that a high asphaltene weight percent was calculated during static experiments (i.e., using filter membranes), and this increase was severe on smaller pore size structures. Dynamic tests (i.e., using shale cores) showed that miscibility increased oil recovery, but a stronger intermediate-wet system was observed when measuring the wettability of cores after N_2 cyclic tests. When starting with shorter soaking times, more oil recovery could be achieved. Oil recovery reduction and asphaltene depositions were observed at later cycles. Microscopy and scanning electron microscopy (SEM) imaging of the Eagle Ford cores showed asphaltene clusters inside the cores after cyclic tests. A mercury porosimeter emphasized the degree of pore plugging after cyclic tests, and the findings revealed a smaller pore size distribution after N_2 tests due to the asphaltene deposition process when compared to cores that had not been pressured. This extensive study focuses on the effects of asphaltene deposition on oil recovery under cyclic N_2-miscible and immiscible conditions in shale resources.

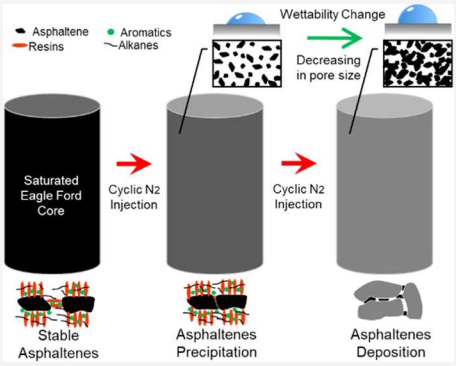

1. INTRODUCTION

Gas injection has been a widely used technology for increasing oil production in unconventional shale plays in the United States, and it may be the most efficient approach for unlocking the remaining oil percentage. Unconventional resources, like shale reservoirs, are widely recognized for their extremely low permeability and porosity.[1] Despite the fact that multistage hydraulic fracturing and horizontal well drilling techniques are used to extract the remaining oil from such reservoirs, only 4−6% of the trapped oil can be extracted, and the oil production drops after a few months, attributing to the ultralow permeability.[2−19] Water injection is also one of the suitable strategies for increasing oil recovery from conventional reservoirs; nevertheless, due to weak injectivity, insufficient sweep potency, and clay swelling concerns, this approach is not the ideal solution for tight reservoirs.[20,21] Cyclic gas injection outperforms gas flooding methods in terms of enhancing oil recovery, mainly in ultratight reservoirs.[22,23] The total organic carbon (TOC) is the most important influencing parameter on gas injection in tight reservoirs because kerogen makes the surface of the pore oil-wet, making the oil inside challenging to extract.[24] Due to the combination of multiphase fluids (i.e., gas, oil, condensate, and water) and scales, multiphase flow production can create a number of challenges including wax and asphaltene deposition, hydrate formation, slugging, and emulsions.[25] Organic hydrocarbon particles settling in oil and gas reservoirs might create many flow assurance problems throughout the extraction process. These materials may increase flow resistance, causing production reduction or even pipeline plugging.[26,27] Crude oil is a complicated composition of hydrocarbons with different molecular weights

Received: July 29, 2022
Revised: September 27, 2022
Published: October 11, 2022

Downloaded via MISSOURI UNIV SCIENCE & TECHNOLOGY on November 28, 2022 at 22:01:12 (UTC).
See https://pubs.acs.org/sharingguidelines for options on how to legitimately share published articles.

ACS Publications

© 2022 American Chemical Society

and organic components such as asphaltenes and wax. Asphaltene is a solid phase in crude oil that is soluble in toluene but insoluble in light *n*-alkanes like *n*-pentane or *n*-heptane.[28] The injected gas reacts with the oil in the shale reservoir, causing the asphaltene inside the crude oil to become more unstable. Throughout most of the gas injection process, the gas alters the composition of crude oil, causing the oil's solubility to change. As a result of the instability of the colloidal suspension in crude oil, asphaltene tends to precipitate and flocculate.[29,30] Asphaltene can negatively affect the permeability of formations by plugging or adsorption.[31] One of the most challenging issues in the shale gas injection process is asphaltene precipitation and deposition, which causes shale pore plugging and wettability changes in the formation.

Because of the impact of asphaltene aggregation during gas injection, several studies have been conducted focusing on cyclic gas injection in conventional reservoir cores.[32−37] Others investigated the stability of asphaltene under carbon dioxide (CO_2) gas injection and different factors were studied.[38−42] CO_2 can evaporate more hydrocarbon components and condensate at a higher concentration into crude oil than N_2, resulting in more asphaltene depositions.[43] There have been very little studies employing N_2 gas injection to illustrate the severity of asphaltene deposition and precipitation as well as the factors influencing its stability.[44−49] Jamaluddin et al.[44] examined the asphaltene stability by contacting various molar concentrations of N_2 with the reservoir fluids and the findings revealed that increasing the concentration of N_2 negatively impacted the instability of asphaltene and increased the quantity of bulk precipitated asphaltene. Zadeh et al.[45] designed an experimental study to evaluate the effect of N_2 and methane on asphaltene precipitation under high-pressure and high-temperature conditions. Their findings demonstrated that asphaltene precipitation was higher under N_2 gas injection than under methane, and temperature had less impact compared to pressure and gas concentrations. Moradi et al.[46] used the high-pressure filtration technique to study asphaltene particle precipitation, aggregation, and breakup using natural depletion and miscible N_2 injection processes. The results showed that N_2 severely destabilizes asphaltenes, and the issue was worsened in heavier crude samples. Khalaf and Mansoori[47] conducted a simulation study to highlight the impact of using miscibilized air and N_2 on asphaltene aggregation. They claimed that the aggregations of asphaltene influenced by the concentration of the injected gas and the difference between asphaltene aggregations using air and N_2 were not significant. Elturki and Imqam[48] conducted an experimental study to investigate the effect of miscible and immiscible N_2 injections on asphaltene deposition using filter paper membranes. They found that miscibility of N_2 resulted in a high asphaltene weight percentage, especially in smaller pore structures.

Most of the reported studies of cyclic injection enhanced oil recovery (EOR) were implemented extensively using CO_2 in shale and tight reservoirs[49−64] and others used lean gas, methane, rich gas, or gas mixture.[65−69] Very little research was conducted using cyclic N_2 injection.[70−75] Yu and Sheng[70] conducted an experimental study using N_2 and Eagle Ford shale cores. They soaked the cores in mineral oil before conducting the experiments. Their findings revealed that N_2 was efficient in improving oil recovery with the majority of oil produced within the first 2 h of production time during the puff stage. Their study's weakness was that they employed mineral oil rather than crude oil, which ignores the influence of asphaltene precipitation on oil recovery. Altawati[71] saturated several Eagle Ford cores with decane oil and 15% NaCl brine water to study the effect of water saturation on oil recovery, utilizing the cyclic CO_2 and N_2 processes. The findings concluded that the partially saturated cores with water gave less recovery factor (RF) compared to cores with no water. The drawback of this study is ignoring the impact of asphaltene deposition. Li et al.[72] investigated the effect of the minimum miscibility pressure (MMP) on oil recovery during the CO_2 cyclic process. They estimated the MMP for a Wolfcamp crude oil using the slim tube method. Wolfcamp cores were used in all of the 15 experiments conducted, and the results showed an increase in oil recovery when inducing a pressure higher than the MMP. Tovar et al.[76] conducted several experiments using 11 Wolfcamp shale cores to investigate the effect of CO_2 and N_2 injection on oil recovery. They investigated various factors including MMP, soaking time, and injection-gas composition. The results showed that CO_2 injection led to more oil recovery compared to N_2 because CO_2 had the ability to vaporize more hydrocarbon components. Higher pressure and longer soaking time led to higher oil recovery even beyond miscibility conditions for CO_2. Bougre et al.[77] conducted an experimental investigation to study the effect of flooding with CO_2, N_2 and a CO_2−N_2 mixture on oil recovery in tight formations. The same core sample was used in all experiments and saturated with live oil from the Eagle Ford formation. For each trial, the sample was cleaned and resaturated. Their results showed higher oil recovery during CO_2 gas injection followed by the N_2−CO_2 mixture with longer breakthrough time. To sum up, a review of the literature shows that the impact of asphaltene due to N_2-miscible injection was not considered; hence, the oil recovery results due to the cyclic injection of N_2 are questionable. Lately, the asphaltene deposition process in tight reservoirs has gained attention during CO_2 cyclic gas injection.[78−83] To the best of our knowledge, no investigations or published work have focused on asphaltene aggregation and deposition under cyclic N_2 injection in tight and shale reservoirs.

Despite the fact that the aforementioned studies investigated various factors affecting the oil recovery from shale reservoirs during continuous and cyclic gas injection processes, there is a lack of a rigorous investigation on how asphaltene deposition impacts the oil recovery in shale reservoirs under miscible and immiscible N_2 cycle processes. This research extends the previous work conducted by Elturki and Imqam,[49,84] which investigated the impact of continuous immiscible and miscible N_2 injections on asphaltene precipitation. The research then studies the severity of asphaltene deposition in unconventional reservoirs due to cyclic miscible and immiscible N_2 gas injections. This extensive study provides a better knowledge of the parameters that influence asphaltene instability during N_2-miscible and immiscible injections in unconventional reservoirs.

2. MATERIALS AND METHODOLOGY

The laboratory work was divided into three sections: (1) MMP determination experiments, (2) cyclic gas injection experiments (using both filter paper membranes and shale cores), and (3) asphaltene pore plugging analysis. The first experiments established the MMP for N_2. Based on the MMP experiments, miscible and immiscible pressures of cyclic gas injection experiments were determined. This step was critical to ensure that the miscibility and immiscibility of the injected gas would be studied in terms of oil recovery and asphaltene pore plugging. Further analysis of the shale

https://doi.org/10.1021/acs.energyfuels.2c02533
Energy Fuels 2022, 36, 12677−12694

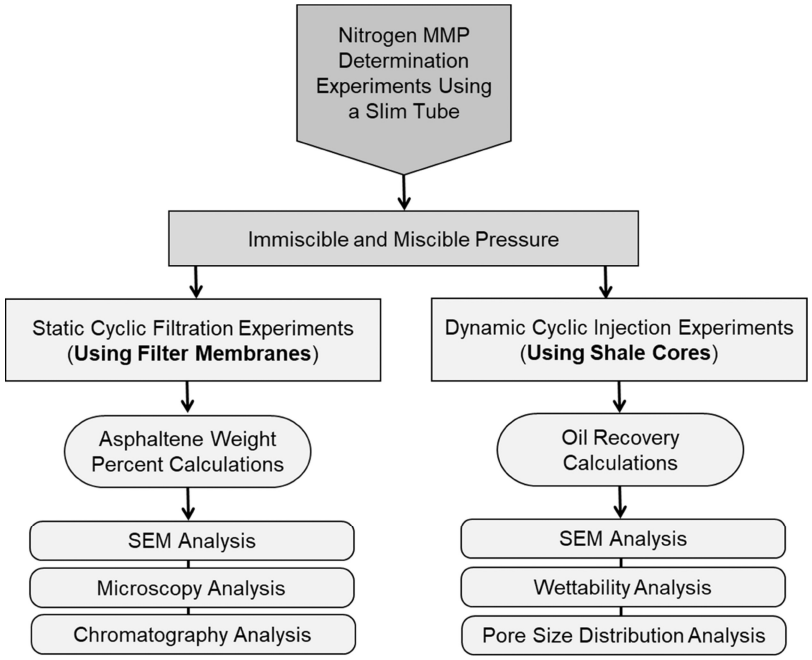

Figure 1. Experimental design flowchart.

cores after the cyclic gas injection experiments used scanning electron microscopy (SEM), wettability measurements, and pore size distribution measurements to highlight the severity of asphaltene deposition on pore plugging during N_2-miscible and immiscible gas injection. Figure 1 shows the experimental flowchart for the main experiments and analyses in this paper. The main materials and their supplier used in this study are summarized in Table 1. Details of the materials used in each experiment will be discussed in the following sections.

Table 1. List of Suppliers of the Main Chemicals/Materials Used in This Study

material	supplier
n-heptane (chemical formula: C_7H_{16}, purity: ≥99%)	Lab Alley Powering
crude oil	Western Missouri Oil Field
Whatman 2.7 μm filter paper	OFITE, Inc.
filter paper membranes (sizes of 50, 100, and 450 nm)	Foxx Life Sciences, Fisher Scientific

The Eagle Ford shale outcrops were saturated with crude oil at 70 °C "158°F" with a viscosity of 19 cp, density of 0.864 g/cm^3, and °API of 32. The viscosity was measured using a rheometer, and gas chromatography–mass spectrometry (GC–MS) was utilized to determine the composition of the crude oil, as shown in Table 2. The crude oil was used in the slim tube experiments with N_2 to determine the MMP. For the cyclic filtration experiments, filter paper membranes of 450, 100, and 50 nm were used. N_2 gas cylinders of 99.9% purity were the source of gas injection to perform the slim tube and cyclic experiments. A specially designed high-pressure, high-temperature vessel (L: 15.24 cm "0.50 ft", ID: 5 cm "0.164 ft", OD: 7.62 cm "0.25 ft") was employed to accommodate the cores during the cyclic experiments. An oven (model LBB2-27-2, Dispatch) was used to adjust the temperature during the MMP experiments. As shown in Figure 2, core samples from Eagle Ford shale outcrops were used in the gas cyclic experiments, with diameter and length of 1 and 2 in, respectively. The average helium porosity was 5.7%, and the average permeability was 198 nD (0.000198 mD). X-ray diffraction (XRD) analysis of the cores is presented in Table 3. The total organic carbon (TOC) of the cores was 5.5%, determined via Rock-Eval pyrolysis.

Table 2. Crude Oil Composition

composition	mass %
C_1	0.000
C_2	0.000
C_3	0.000
C_4	0.003
C_5	0.063
C_6	0.430
C_7	0.540
C_8	64.484
C_9	0.278
C_{14}	0.309
C_{15}	0.349
C_{16}	0.425
C_{17}	3.490
C_{18}	0.196
C_{19}	1.166
C_{20}	3.596
C_{21}	0.926
C_{22}	2.662
C_{24}	1.973
C_{27}	5.395
C_{28}	7.225
C_{29}	1.322
C_{30+} (including asphaltene)	5.17
total	100

Before the saturation process, 12 shale core samples were named and weighed with the same crude oil from the MMP experiments. An accumulator filled with crude oil was used to accommodate the shale cores, after which high pressure was injected along with high temperature from an oven being applied for 10 continuous months to ensure that the core samples are well saturated. The justification for discontinuing the experiment after 10 months was that the weight of the cores had not changed in the last 2 months of the saturation

https://doi.org/10.1021/acs.energyfuels.2c02533
Energy Fuels 2022, 36, 12677−12694

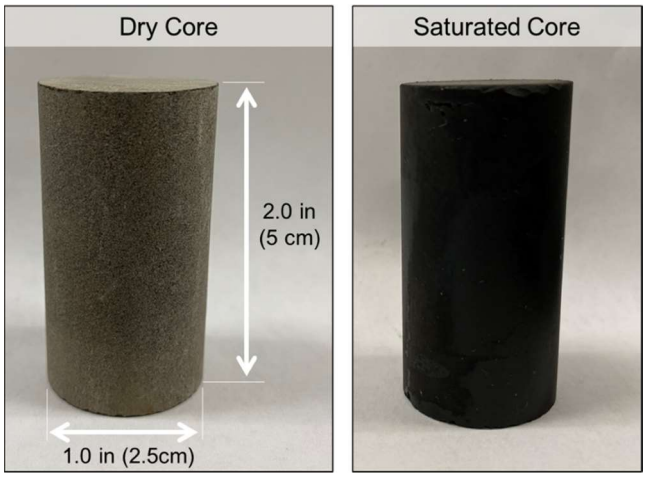

Figure 2. Sample of an Eagle Ford core plug before and after the oil saturation process.

Table 3. Eagle Ford XRD Results

mineral	calcite	quartz	dolomite	pyrite	kaolinite
composition (%)	70	18	2	1	9

process, indicating that the cores had been saturated. Examples of the weight change during the saturation process are shown in Figure 3.

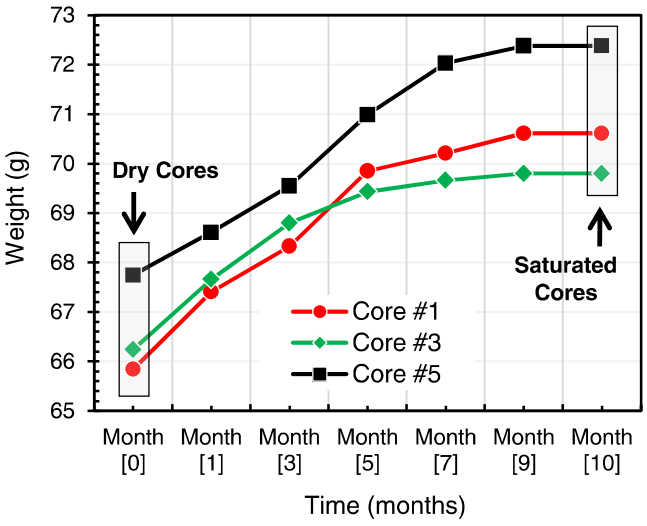

Figure 3. Three examples of core saturation process during a 10-month period.

2.1. Slim Tube Experiments for MMP Determination. A slim tube (L: 1310 m "42.97 ft", ID: 0.21 cm "0.0068 ft", OD: 0.41 cm "0.0134 ft") packed with sand was used to perform the experiments along with three accumulators. The permeability of the sand pack is 27.50 Darcy. Figure 4 shows the main components of the slim tube apparatus. The three main steps in slim tube experiments are (1) slim tube cleaning, (2) saturation of the slim tube with crude oil, and (3) gas injection. Therefore, accumulator 1 contained the crude oil to saturate the slim tube; accumulator 2 was filled with a solvent of *n*-heptane to clean the slim tube; and accumulator 3 was filled with gas to be injected into the slim tube during the experiments. The procedure to conduct the experiments started with the slim tube, which was fully saturated with distilled water. Next, oil was injected into the slim tube at a rate of 0.25 mL/min until fully saturated. This can be observed at the outlet of the slim tube when the produced liquids were only oil, thus ensuring that the slim tube was fully saturated. During all of the experiments, a back pressure regulator was placed at the outlet with the desired pressure. The gas accumulator was filled with N_2. Then, gas was injected at a predetermined pressure using the constant pressure mode of the syringe pump. Each experiment was stopped when 1.2 PV of gas had been injected or when the gas broke through. The produced oil was collected from the effluent. The MMP can be determined by plotting the gas injection pressure versus the cumulative oil recovery. Finally, after each experiment, the solvent xylene was used to clean the slim tube setup and guarantee that no oil remained in the slim tube to impact the following experiment.

2.2. Gas Cyclic Experiments Using a Filtration Technique (Static Mode). Figure 5 illustrates the main components of the cyclic gas process utilizing filter paper membranes. The main principle of filtration experiments is to understand the asphaltene deposition in a controlled pore size structure and the factors that may impact the process that then give an idea about the process when using real shale cores. The primary component was a high-purity N_2 cylinder with pressure regulators to adjust the cylinder pressure. Because the outlet pressure of the N_2 cylinder was limited, a gas accumulator was utilized to collect the gas and inject it into the vessel using a syringe pump to achieve higher pressures if needed. Filter paper membranes (i.e., 50, 100, and 450 nm) were employed to mimic the shale reservoir structure and to investigate the effect of various pore sizes. A high-pressure high-temperature filtration vessel was designed to accommodate three mesh screens to support the filter membranes and prevent them from folding under high pressure. The mesh screens were designed with small holes that allowed the oil to pass through easily. Spacers between each mesh screen were added to support each screen in place, and rubber O-rings were placed above and below each spacer to prevent leakage and to ensure that the oil and gas would pass through the filter paper membranes. The injection and production lines were located on the top of the vessel for the cyclic technique. Finally, one transducer was installed on the top of the filtration vessel and connected to a computer to monitor and accurately record the injection pressure. The following procedure was followed to conduct the cyclic gas injection experiments using the filtration technique:

- The filter paper membranes were placed inside the vessel in the following order: 50 nm at the bottom, 100 nm in the center, and 450 nm at the top. Mesh screens and spacers supported all filter paper membranes.
- The vessel was then sealed and connected to the system and the gas cylinder.
- The gas cylinder was opened to fill the gas accumulator. Then, the gas cylinder was closed using a pressure regulator.
- Crude oil (30 mL) was pumped into the vessel using a syringe pump linked to the oil accumulator, after which the gas was injected into the vessel at the predetermined pressure.
- The gas was allowed to interact with the crude oil inside the vessel for a predetermined soaking time (i.e., 6 h); this step is referred to as the "huff" stage.
- A heating jacked was turned on around the vessel to increase the temperature to the desired level (i.e., 70 °C).
- The vessel was depressurized after completing the soaking time. This step is referred to as the "puff" stage.
- The produced oil was collected from the effluent, after which the vessel was opened, and a sample of the filtered crude oil was collected from each filter membrane for asphaltene analysis. Then, the collected filtered oil on each filter paper membrane was returned carefully for a new cycle.
- All of the above steps were repeated for a new cyclic process without changing the filter membranes.

The oil samples (1 mL) obtained from each filter membrane were mixed in test tubes after each cycle with the solvent *n*-heptane (40 mL) at a ratio of 1:40 for asphaltene weight percent measurements. After the asphaltene was fully deposited in the test tube, the mixture was filtered using filter paper (2.7 μm). Weighing the filter paper before and after the filtration process quantified the asphaltene weight

https://doi.org/10.1021/acs.energyfuels.2c02533
Energy Fuels 2022, 36, 12677−12694

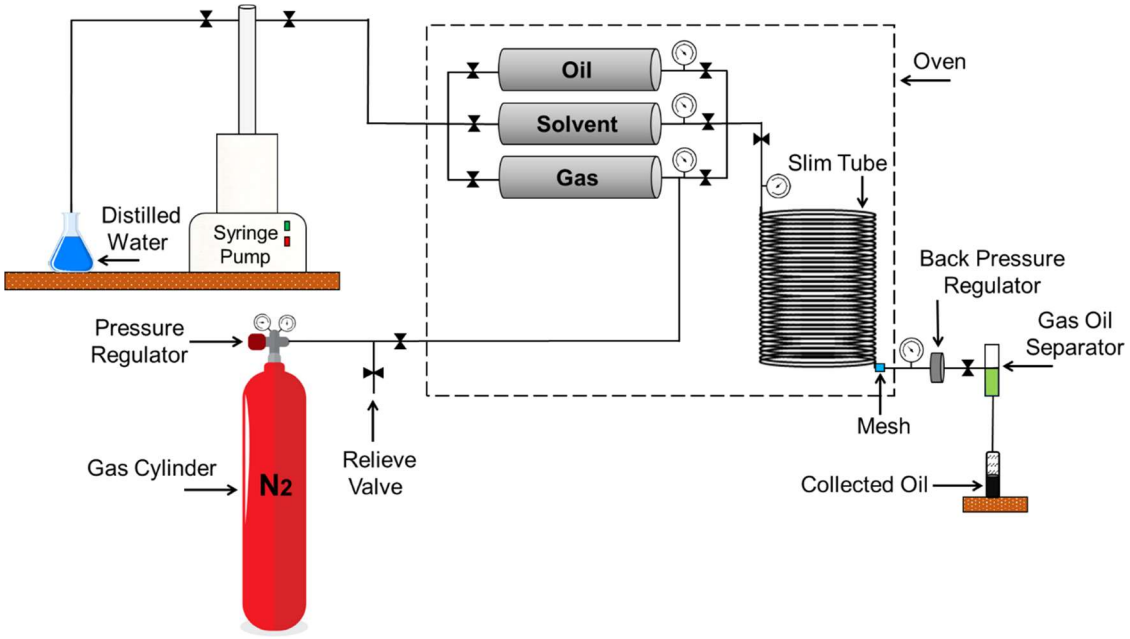

Figure 4. Schematic of the setup of the N_2 MMP determination apparatus using the slim tube technique.

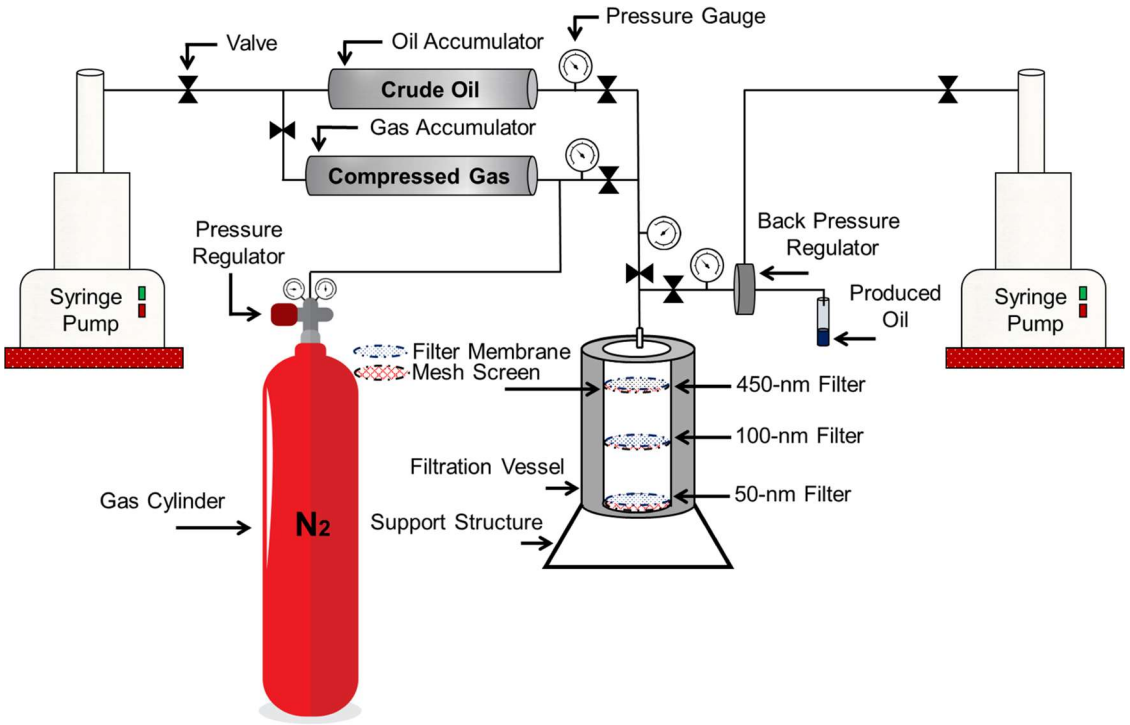

Figure 5. Illustration of the cyclic filtration test setup.

percent. Using the following equation, the difference between these weights determined the asphaltene weight percent

$$\text{asphaltene wt \%} = \frac{\text{wt asphaltene}}{\text{wt oil}} \times 100 \quad (1)$$

where asphaltene wt % is the asphaltene weight percent, wt asphaltene is the asphaltene weight on the filter paper, and wt oil is the oil sample weight.

2.2.1. Scope of the Work for the Cyclic Filtration Technique. In one part of the research, four filtration experiments were designed to investigate the effect of gas injections on asphaltene in crude oil, including two experiments using two conditions (i.e., miscible and immiscible), with the pressures selected based on previous MMP experiments. All of the experiments were conducted at 70 °C to mimic the reservoir temperature, with a fixed soaking time of 6 h. These experiments were designed to provide a comprehensive evaluation of how each gas would impact the pore structure of the filter paper membranes (which represent shale unconventional reservoirs). The operating conditions are presented in Table 4.

2.3. Gas Cyclic Experiments Using Shale Cores (Dynamic Mode). Based on the results of the MMP, eight experiments were conducted on eight Eagle Ford core samples at pressures above and below the N_2 MMP. The apparatus employed in the cyclic experiments is shown in Figure 6. A top view of the real vessel is

https://doi.org/10.1021/acs.energyfuels.2c02533
Energy Fuels 2022, 36, 12677−12694

Table 4. Operating Conditions for the Cyclic Filtration Tests at Miscible and Immiscible Gas Injections

test no.	pore size of filter membrane (nm)	gas injected	soaking time (h)	injection pressure (psi)	pressure condition
1	450	nitrogen (N_2)	6	1000	immiscible
	100				
	50				
2	450		6	1750	miscible
	100				
	50				

shown in Figure 7. The core was placed inside the vessel above a mesh screened plate to let the gas to spread around the core more effectively. The main components were a gas cylinder as the source of the gas injection, a stainless steel high-pressure vessel to accommodate the core, a syringe pump connected to the gas accumulator for storing the injected gas and increasing the pressure, and a heat jacket to mimic the temperature conditions in an actual tight reservoir.

The following procedure was followed to conduct the cyclic gas injection experiments.

- The saturated core was placed inside the vessel.
- The vessel was connected to the high-pressure gas cylinder and the gas accumulator; then, the vessel was secured.
- The gas was injected into the vessel at the designed pressure, and then the gas was allowed to interact with the saturated core for a predetermined time (soaking period). This step is also called the huff stage.
- A heating jacked was turned on around the vessel to increase the temperature to the desired level.
- After the soaking time was completed, the vessel was depressurized (puff stage).
- The shale core was retrieved to calculate the oil recovery at specific production times using the change in weight method described in the following equation

$$\text{oilrecoveryfactor} = \frac{wt_1 - wt_2}{wt_1 - wt_{dry}} \quad (2)$$

where wt_1 is the weight of the saturated core, wt_2 is the production time core weight, and wt_{dry} is the weight of the cores before the saturation process.

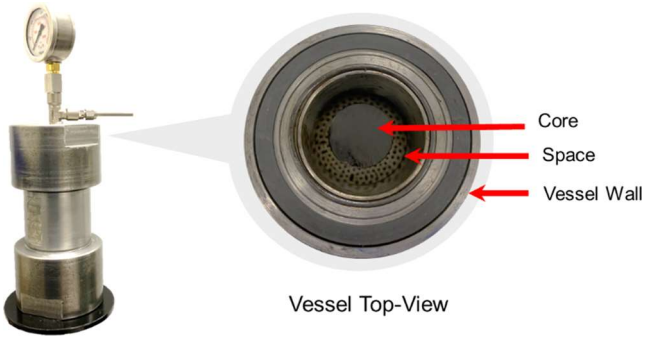

Figure 7. Top view of the real vessel.

- A new gas cycle was conducted after measuring the oil recovery from the previous cycle, and the cycles were stopped when there was no oil recovery from the saturated core.
- After finishing the experiments, the shale cores were analyzed for asphaltene deposition, pore size distribution changes, and wettability alteration.

2.3.1. Scope of the Work for the Gas Cyclic Process Using Shale Cores. In this part of the experiment, eight Eagle Ford shale cores were used to conduct cyclic gas injection experiments to investigate the effect of miscible and immiscible conditions for N_2 on oil recovery and asphaltene deposition. An additional four saturated cores were not exposed to gas injection and served as references (constants) to determine the wettability and pore size distribution before conducting the cyclic experiments. The effects of soaking time, production time, and injection pressure were analyzed. The operation conditions are presented in Table 5. Gas injection experiments were conducted using eight shale cores each of which was exposed to different N_2 injection pressures. To study the effect of the soaking time on oil recovery, different cores underwent a gas cyclic pressure of 2000 psi and various soaking times (i.e., 1, 6, 12, and 24 h). The soaking time was investigated in two ways: using one core for all soaking times (test no. 5) and using different cores for each soaking time (test nos. 6−8) to highlight the effect of resoaking gas injections on oil recovery. (Note: this will be explained in the soaking time mode section in the results section.) All of the experiments were conducted at 70 °C to mimic the reservoir temperature. In each experiment, the number of cycles was different, but the cycles were stopped when no more oil recovery

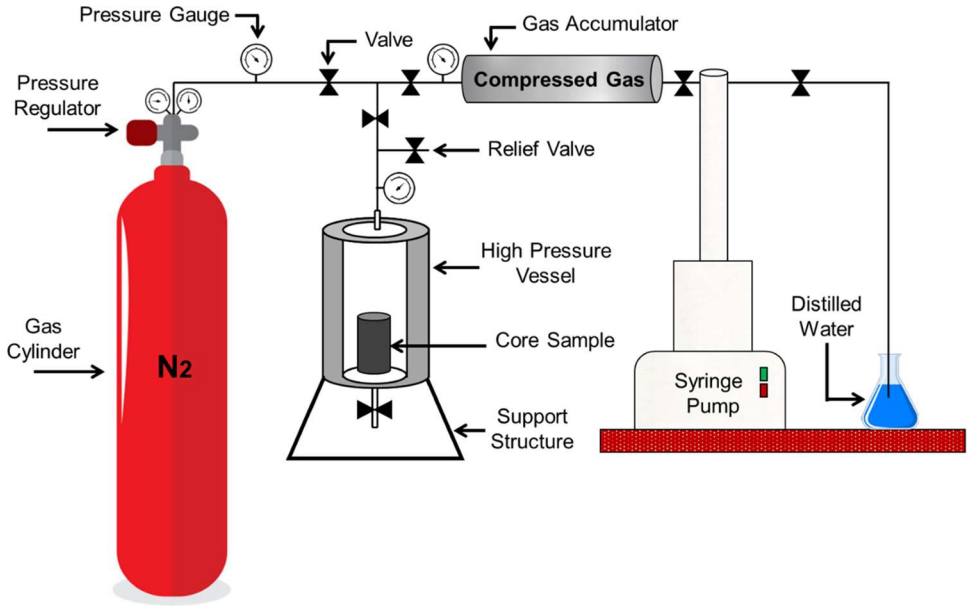

Figure 6. Cyclic experimental setup.

https://doi.org/10.1021/acs.energyfuels.2c02533
Energy Fuels 2022, 36, 12677−12694

Table 5. Operating Conditions for N_2 Cyclic Tests at Miscible and Immiscible Gas Injections[b]

test no.	core no.	gas injected	soaking time (h)	injection pressure (psi)	production time (min)
1	#1	nitrogen (N_2)	6	1000	15, 60, and 90
2	#2		6	1300	
3	#3		6	1750[a]	
4	#4		6	2000[a]	
5	#5		1, 6, 12, and 24	2000[a]	15
6	#6		1	2000[a]	
7	#7		12	2000[a]	
8	#8		24	2000[a]	

[a]Injected gas in miscible condition. [b]Note: Four more cores served as references for the wettability measurement and pore size distribution determinations, with the cores numbered #9, #10, #11, and #12.

occurred. The production times (i.e., the time at which the core was weighed after completing the gas cycling) were selected to be 15, 60, and 90 min for both miscible and immiscible conditions. The miscible and immiscible pressures were selected based on the slim tube experiments.

3. RESULTS AND DISCUSSION

3.1. MMP Results. Minimum miscibility pressure (MMP) can be defined as the lowest pressure at which a gas can create miscibility with the reservoir oil at the reservoir temperature.[85] To investigate the effect of miscibility on oil recovery and its impact on asphaltene deposition in shale cores during cyclic gas injection, seven experiments were conducted at pressures of 500, 750, 1000, 1250, 1500, 1750, and 2000 psi at 32 and 70 °C, as shown in Figure 8. MMP experiment was conducted at

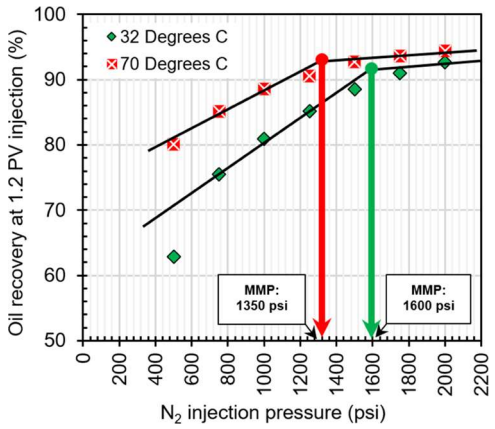

Figure 8. MMP determination using an oil viscosity of 19 cp at 32 and 70 °C.

32 °C as a reference and to ensure the accuracy of the MMP results. Table 6 shows the cumulative oil recovery at each injected pressure for N_2. The N_2 MMP pressures were determined to be 1600 and 1350 psi at 32 and 70 °C, respectively. The results demonstrated that the MMP of N_2 was decreased when increasing the temperature due to the N_2 remaining in the gaseous phase at the same conditions and higher intermediate components of the oil.[86−90] Based on the MMP results, miscible and immiscible pressures were selected to conduct the cyclic gas experiments and will be discussed in the next section.

3.2. Results of the Gas Cyclic Experiments Using a Filtration Technique. Two sets of cyclic experiments were conducted using the cyclic filtration technique. An immiscible pressure of 1000 psi and a miscible pressure of 1750 psi were used to evaluate asphaltene instability under immiscible and miscible scenarios. The soaking time was fixed at 6 h, and the temperature was 70 °C. Figure 9 shows the results of N_2 cyclic filtration experiments, demonstrating that asphaltene in crude oil was altered at different degrees of aggregations by N_2 in the first two cycles in all of the filter paper membranes. For the immiscible N_2 pressure of 1000 psi, the asphaltene weight percent increased slightly in 450 nm filter from 5.56 to 5.84% from the first to second cycles, respectively. The asphaltene weight percent increased slightly as the number of cycles increased until it started to stabilize in the fifth cycle, which indicated that the asphaltene clusters and particles were impacted at a higher rate in the earlier cycles. A higher asphaltene weight percent was observed on the 50 nm filter due to its smaller pore size structure. In 50 nm filter, the asphaltene weight percent increased from 9.16 to 11.88% for the first and the fourth cycles, respectively. In the fifth cycle, the asphaltene weight precent increased slightly to 12.20% and then stabilized. On the other hand, the miscible N_2 pressure of 1750 psi increased the asphaltene weight percent much more in all the filter paper membranes, which revealed that miscibility had significantly weakened the bonds between the asphaltene clusters and resins inside the crude oil. For instance, the asphaltene weight percent in the 50 nm filter in the first cycle was 20.19% and then increased significantly to 26.73% in the fourth cycle. Then, the asphaltene weight percent was almost stable at 27.46% in all of the next cycles. In summary, for all cyclic tests, asphaltene weight percent increased as the pore size of the filter membranes decreased, and the number of gas injection cycles increased. The results showed that the miscible N_2 pressure causes more asphaltene challenges, according to these findings, especially in smaller pores. The mass transfer ability (i.e., evaporation of light components) of miscible conditions is stronger. The extraction of light components in crude oil was higher during miscible N_2 injection and could result in more heavy components[76,91]

Table 6. N_2 Slim Tube Cumulative Oil Recoveries (%)

tested injected pressure (psi)	500	700	1000	1250	1500	1750	2000
cumulative OR at 32 °C	62.92	75.51	80.96	85.15	88.51	91.03	92.71
cumulative OR at 70 °C	80.12	85.15	88.51	90.61	92.71	93.54	94.38

https://doi.org/10.1021/acs.energyfuels.2c02533
Energy Fuels 2022, 36, 12677−12694

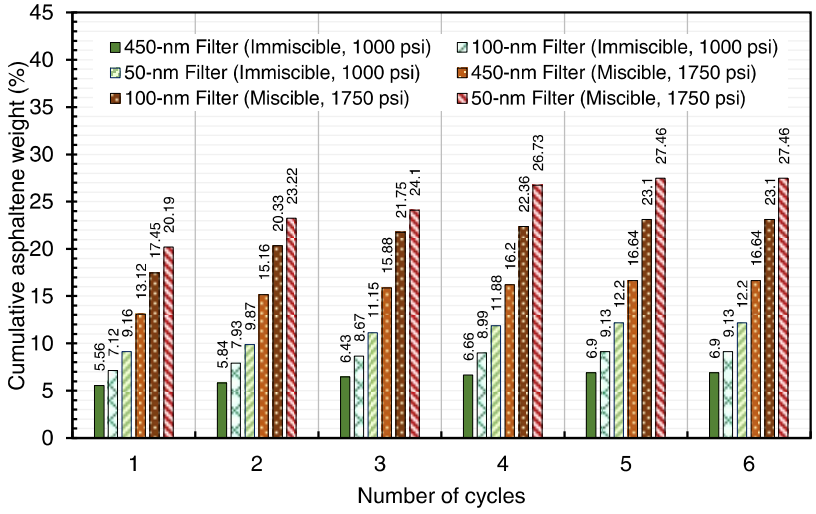

Figure 9. Asphaltene weight percent in all filter membranes after six immiscible (i.e., 1000 psi) and miscible (i.e., 1750 psi) cyclic N_2 gas injections at 70 °C.

and this explains why the immiscible N_2 had less asphaltene deposition and fluctuations.

3.2.1. Chromatography Analysis Results. After the last injection cycle of filtration experiments, oil samples were collected from the produced oil to evaluate the influence of gas injection on asphaltene stability in crude oil, and then gas chromatography−mass spectrometry (GC6890-MS5973) was used to determine the main chemical components, including asphaltenes. Figure 10 shows the grouped carbon number

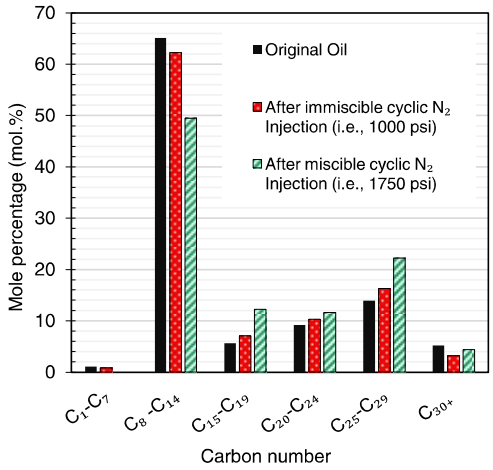

Figure 10. Distribution of oil components before and after N_2 cyclic filtration injections of 1000 and 1750 psi.

distribution of the produced oil following cyclic tests utilizing immiscible and miscible conditions for N_2. The results showed that miscible N_2 injection had a higher impact on the crude oil, which can be seen in the higher mole percentage of the intermediate and heavy components (C_{15}−C_{30}). The light components (C_8−C_{14}) were partially extracted from the original oil due to the high pressure and strong light hydrocarbon extraction of N_2. Following miscible N_2 testing, slightly higher amounts of C_{31+} including asphaltenes were found compared to the initial oil composition, but after immiscible N_2 tests, less heavy components were found because the mass transfer ability of miscible N_2 is much stronger than immiscible N_2. Also, higher pressure during miscibility conditions will weaken the bonds between asphaltene particles and the resin inside the crude oil, and thus more heavy components and asphaltene deposition may occur. In the crude oil, immiscible N_2 has low solubility and thus has a low mass transfer capacity, which might result in less extraction of light hydrocarbons and likely less asphaltene flocculation compared to the miscible N_2 injection pressure.[91−93] Finally, it is worth mentioning that the difference in the heavy components (C_{31+}) after miscible and immiscible injections was not significant due to the fact that the heavy components, including asphaltenes, were not fully deposited on the filter membranes because of small lab-scale experiments. Further research is required to apply these findings to field applications.

3.2.2. Microscopy and SEM Analysis. After completing the filtration experiments, the impact of gas injection and asphaltene clusters on the pore plugging on the filter paper membranes was determined using a Hirox digital microscope. Figure 11 shows the microscopic images (500 μm) of the filter paper membranes' pore structure for the 450, 100, and 50 nm filters using immiscible (i.e., 1000 psi) and miscible (i.e., 1750 psi) N_2 injection pressures. The photos were taken after the filter membranes had been cleaned and exposed to an *n*-heptane solvent for 24 h. For miscible N_2 conditions, the asphaltene particles plugged more in 50 nm areas due to their smaller pore size, which led to greater asphaltene deposition. On the other hand, the filter membranes of 450 nm showed a notable pore plugging and asphaltene clusters, as well as the 100 nm filter paper. Additionally, scanning electron microscopy (SEM) was utilized to obtain high-quality pictures of the pore structure of filter paper membranes for further imaging analysis. Various images (500 μm) were taken for the same size filter membranes (i.e., 450, 100, and 50 nm) during immiscible (i.e., 1000 psi) and miscible (i.e., 1750 psi) N_2 injection pressures at 70 °C, as shown in Figure 12. The photos of the 450 nm filter after N_2 injection showed that asphaltenes plugged the pores and accumulated inside the structure of the filter membranes. This was much more severe in the 50 nm filter due to its small pore size structure. Miscible N_2 injection led to more dark colors in the photos, and more particles were noticed. More details of N2 precipitation on the paper membrane can be found in our previous publications.[49,84]

https://doi.org/10.1021/acs.energyfuels.2c02533
Energy Fuels 2022, 36, 12677−12694

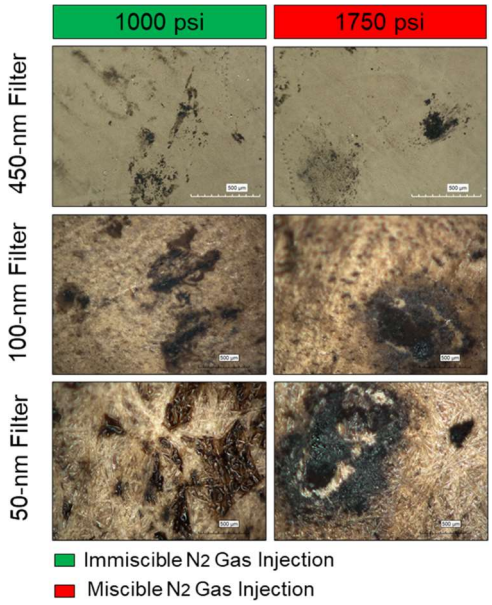

Figure 11. Digital microscopic images (500 μm) of 450, 100, and 50 nm filter membranes after the last cycle of 1000 and 1750 psi N_2 injection pressures.

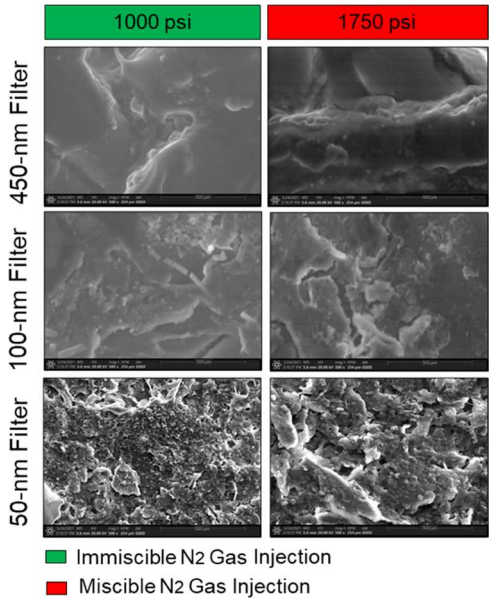

Figure 12. Scanning electron microscopy (SEM) images (500 μm) of 450, 100, and 50 nm filter membranes after the last cycle of 1000 and 1750 psi N_2 injection pressures.

These findings confirm that miscible N_2 has a higher solubility and strong extraction of light hydrocarbons in crude oil compared to immiscible N_2, which could lead to less asphaltene issues.

3.3. Results of Cyclic Gas Injection Using Shale Cores.

3.3.1. Effect of Miscibility on Oil Recovery. In this section, the effect of the cyclic injection pressure on oil recovery was studied using eight Eagle Ford shale cores. To examine the miscibility influence on oil recovery, four sets of experiments (tests 1−4) were performed at pressures below and above the N_2 MMP. Table 7 presents the cumulative recovery factor (RF) data calculated after each cycle of cyclic N_2 tests. In all experiments, the soaking time was fixed at 6 h. The production time was investigated, and oil recovery was measured at different production times (i.e., 15, 60, and 90 min). The cycles were stopped when no oil recovery was produced. The results (Figure 13) indicate that oil recovery was less under immiscible pressures than under miscible pressures. As the pressure increased, the oil recovery increased, which can be observed in the first cycle. The findings also suggested that under both conditions, oil can be extracted effectively in the first four cycles, but no more oil can be extracted after the sixth cycle. For immiscible cyclic N_2 conditions, the essential impact in oil recovery was after the second cycle. Immiscible pressure of 1000 psi had no significant effect in increasing the oil recovery, demonstrating that immiscibility is not the optimum choice when applying the cyclic N_2 techniques. These observations give the miscible pressure an advantage in increasing the oil recovery compared to the immiscible pressure. The key explanation for this is that N_2 injection in miscible conditions has a higher solubility, which reduces the oil's viscosity, increasing the oil recovery as compared to N_2 injection in immiscible conditions, which have a poor evaporation mechanism and oil swelling efficiency. In terms of asphaltene deposition, the figures suggested that it began to affect the oil recovery in the later cycles, as seen by the stable recovery in the last two cycles for all tests. Asphaltene particles began to precipitate mostly in the large pores at lower pressures (i.e., immiscible conditions) and then asphaltenes began to precipitate even in smaller pores[93] under miscible conditions and after multiple cycles. Consequently, the blockage rate increased. These findings imply that oil recovery occurred more during early cycles when asphaltenes had not yet fully developed and plugged the pores of the cores.

During cyclic experiments, we recognized that the production time had an effect on oil recovery; thus, three different production times were considered to determine the oil recovery after each cycle. The production time was the time that had elapsed when the core sample was retrieved from the vessel and weighed. Oil recovery was determined at 15, 60, and 90 min of production time. The soaking time was fixed to be 6 h for each cycle and all of the results are shown in Figure 13. The results revealed that the oil recovery was changed for all production times in all experiments of immiscible and miscible injection conditions. For example, the recovery factor increased slightly during the second cycle from 2.86 to 3.12% during the immiscible pressure of 1000 psi for 15 and 90 min of production times, respectively. During the miscible pressure of 2000 psi, oil recovery was observed in almost all cycles, but less change was determined in the last two cycles. This could be due to the fact that most of the retrievable oil was produced at the miscible pressure and first cycles. The results demonstrated that the production time positively affected the recovery factor during cyclic N_2 tests.

3.3.2. Soaking Time Mode. Two modes of soaking time were conducted at a constant pressure of 2000 psi and fixed production time of 15 min. Mode I refers to conducting several injection cycles at a constant injection pressure (i.e., 2000 psi) on the same core for varied soaking times (i.e., 1, 6, 12, and 24 h), while Mode II refers to using separate cores for a single constant soaking time for each core. One test was conducted for N_2, using the same core for each test (test no. 5). Soaking times of 1, 6, 12, and 24 h were selected and applied to the same core during the tests. Another three tests were conducted using Mode II (test nos. 6−8). Soaking times of 1, 12, and 24 were selected, and the 6 h soaking time results were discussed

https://doi.org/10.1021/acs.energyfuels.2c02533
Energy Fuels 2022, 36, 12677−12694

Table 7. Summary of the Cumulative Recovery Factor (%) Determined after N_2 Cyclic Tests

test no.	soaking time (h)	pressure (psi)	production time (min)	cycle 1	cycle 2	cycle 3	cycle 4	cycle 5	cycle 6	cycle 7
1	6	1000	15	1.81	2.64	3.38	4.63	4.85	4.85	
			60	2.07	2.87	3.67	4.72	5.02	5.02	
			90	2.33	3.13	3.93	5.06	5.28	5.28	
2	6	1300	15	8.88	10.33	11.43	12.03	12.03		
			60	9.42	10.67	11.77	12.37	12.37		
			90	9.71	11.14	12.44	12.64	12.64		
3	6	1750	15	9.08	11.10	12.82	15.24	15.24		
			60	9.80	11.38	13.95	16.36	16.36		
			90	10.53	12.28	14.98	16.95	16.95		
4	6	2000	15	9.12	13.22	17.65	20.33	20.33		
			60	9.55	13.66	18.90	20.59	20.59		
			90	10.00	13.95	19.20	20.87	20.87		
5	1	2000	15	7.61	11.07	12.68	13.14	13.56	14.02	14.00
	6	2000	15	14.10	15.20	16.00	16.19	17.33	18.50	18.50
	12	2000	15	17.20	18.66	21.00	23.65	24.67	26.48	26.48
	24	2000	15	28.32	30.16	32.55	35.84	37.39	40.22	40.22
6	1	2000	15	4.74	5.50	7.23	8.26	10.11	11.12	11.12
7	12	2000	15	9.14	14.80	19.87	22.19	23.50	23.60	23.60
8	24	2000	15	15.12	23.74	29.01	32.71	33.66	33.67	33.67

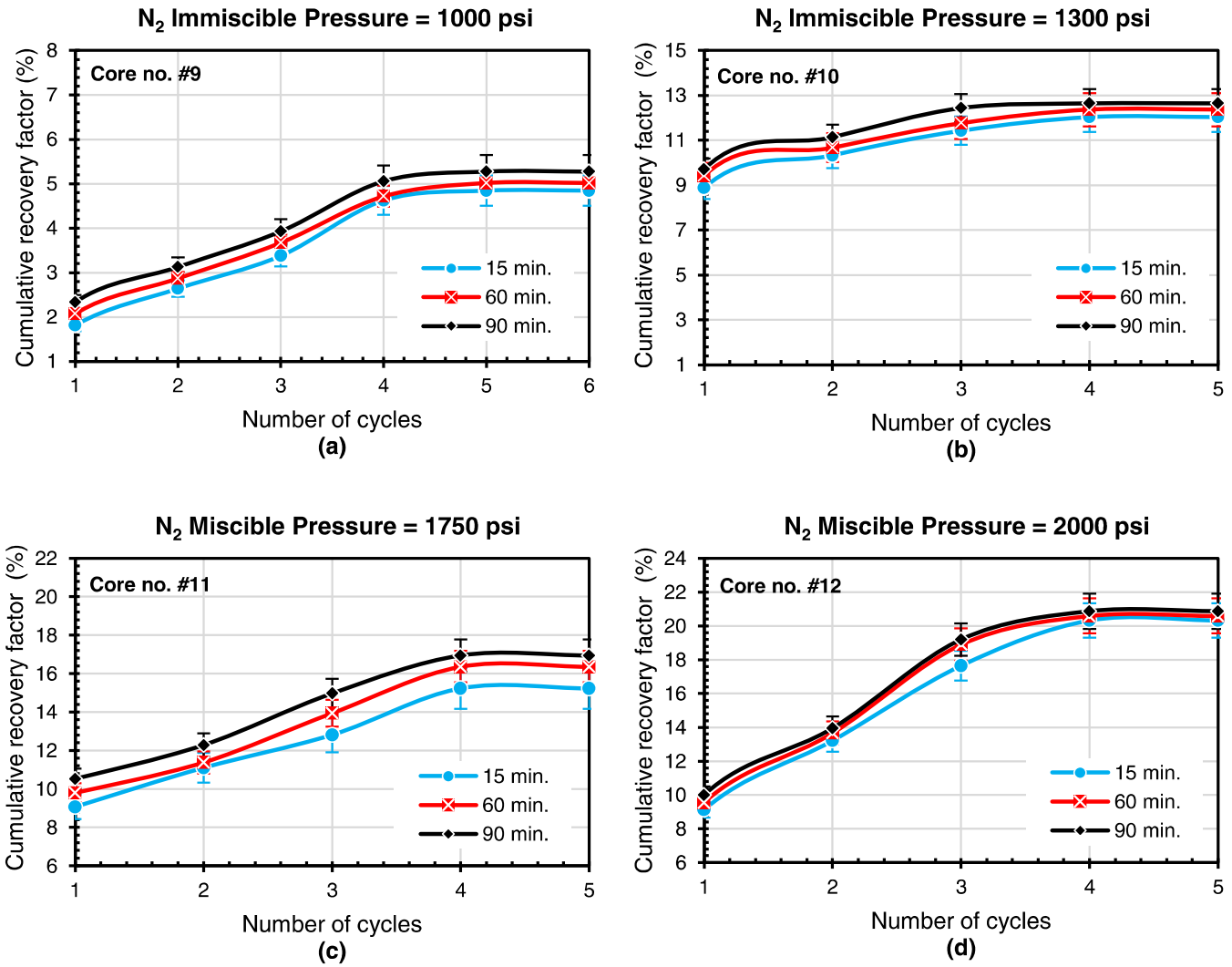

Figure 13. Comparison of recovery performance between immiscible (a and b) and miscible (c and d) N_2 cycles under a 6 h soaking time.

in the previous section. Figure 14 shows an illustration of different soaking time modes.

The results showed that seven cycles were enough to produce more than 40% of the oil using Mode I, as shown in

https://doi.org/10.1021/acs.energyfuels.2c02533
Energy Fuels 2022, 36, 12677−12694

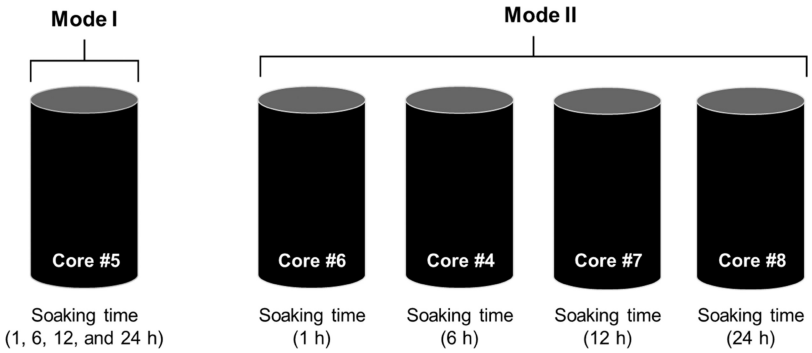

Figure 14. Illustration of different soaking time modes.

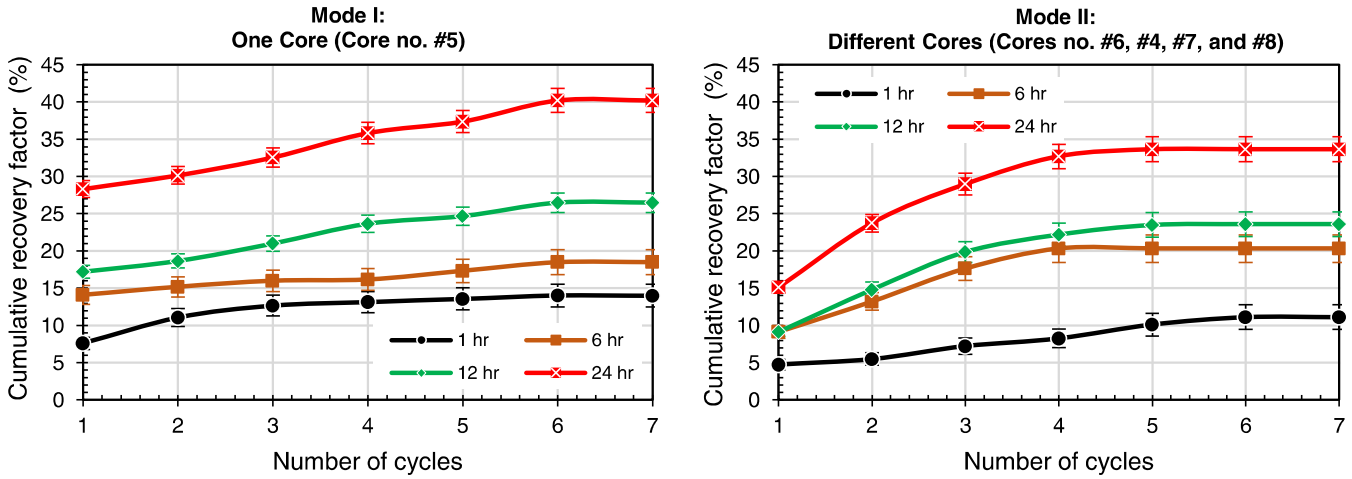

Figure 15. Results of cumulative recovery factor of cyclic N_2 injections using Mode I and Mode II at a 2000 psi cyclic injection pressure with different soaking times.

Figure 15. A soaking time of 24 h produced the highest oil recovery compared to other soaking times of 1, 6, and 12 h. Comparing the results with the oil recovery from Mode II, the highest oil recovery occurred when using a 24 h soaking time where the cumulative oil recovery was about 33.67% after seven cycles. The optimum number of cycles at which no more oil recovery was observed was six. These results demonstrated that longer soaking times lead to higher oil recovery and this process was observed clearly when using Mode I. More hydrocarbons evaporated using Mode I compared to Mode II. The results revealed that starting with shorter cycle time has more advantages in increasing the oil recovery from shale cores as the cyclic gas can condensate at higher concentration in crude oil giving the gas to evaporate more hydrocarbon from the shale cores, especially in miscible conditions. The asphaltene particles did not plug the pores completely, and more oil recovery was obtained. Starting with longer soaking time impacted the asphaltene instability at higher rate inside the cores and thus more pore plugging could exist, resulting in oil recovery reduction, as shown in Mode II using 24 h soaking time. Figure 16 shows the core samples after N_2 cyclic tests after 24 h of soaking time and injection pressure of 2000 psi using Mode I and Mode II.

3.3.3. Wettability Change due to Asphaltene Deposition. In the literature, the contact angle and wettability of shales during N_2 cyclic gas injection are still poorly investigated. During gas injection, asphaltene deposition and precipitation may affect the wettability of shales and hence the effectiveness of oil recovery. Due to the ultralow permeability of the shale

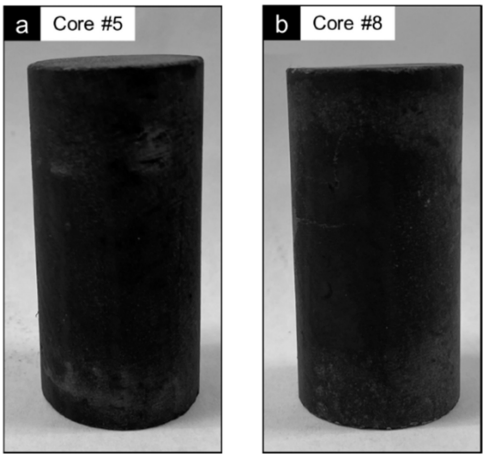

Figure 16. Photos of cores taken after cyclic gas injection experiments at a pressure of 2000 psi (a) after a N_2 test using Mode I and (b) after a N_2 test (24 h soaking time) using Mode II.

structure, the capillary pressure in shale rocks is extremely high. The tendency of fluids to adhere to the surface is known as the wettability phenomenon.[94] Wettability alterations during gas-enhanced oil recovery, especially in unconventional reservoirs, are a significant factor in oil production. The wettability of shale rocks differs; it can be wet with water or oil, and it is not always oil-wet as is usually assumed.[95] However, other investigations reported that shale rocks are more oil-wet.[96,97] Wettability is influenced by the adsorption of

https://doi.org/10.1021/acs.energyfuels.2c02533
Energy Fuels 2022, 36, 12677−12694

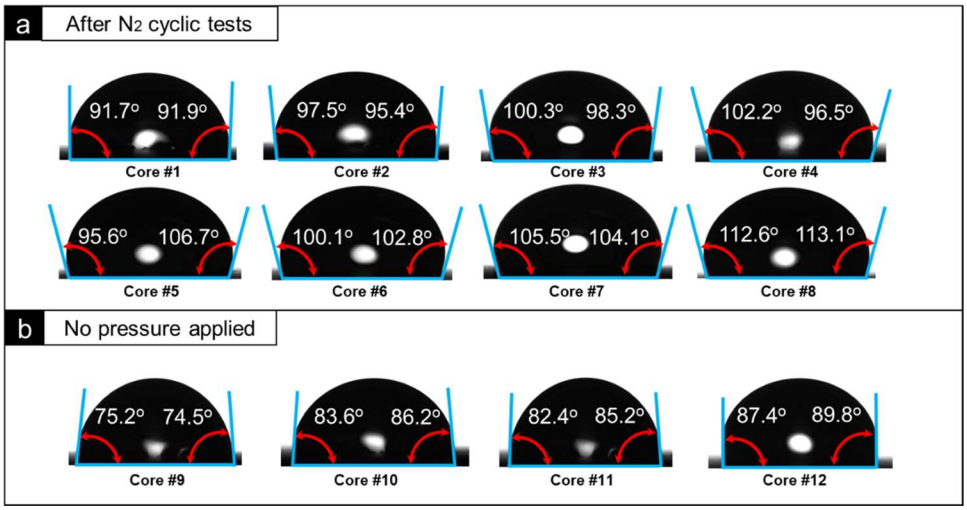

Figure 17. Equilibrated droplets of brine on different core samples and their contact angles (a) after N_2 cyclic tests and (b) no pressure applied on cores.

Table 8. Contact Angle Measurements for all Cores in This Study

stage	condition	test no.	pressure (psi)	average contact angle (deg)	wettability status[a,b]	total average
before cyclic tests			no pressure applied	83.80	weakly intermediate-wet	82.95
				74.50	weakly intermediate-wet	
				88.60	weakly intermediate-wet	
				84.90	weakly intermediate-wet	
after nitrogen cyclic tests	immiscible	1	1000	91.80	strongly intermediate-wet	100.26
		2	1300	96.45	strongly intermediate-wet	
	miscible	3	1750	99.30	strongly intermediate-wet	
		4	2000	99.35	strongly intermediate-wet	
		5	2000	101.15	strongly intermediate-wet	
		6	2000	101.45	strongly intermediate-wet	
		7	2000	104.80	strongly intermediate-wet	
		8	2000	107.85	strongly intermediate-wet	

[a]Classification based on definitions adopted from Anderson[109] and Arif et al.[110] [b]Wettability is classified as follows: 0° = completely water wet; 0−50° = strongly water wet; 50−70° = weakly water wet; 70−90° = weakly intermediate-wet; 90−110° = strongly intermediate-wet; 110−130° = weakly oil-wet; and 130−180° = strongly oil-wet.

asphaltenic components as well as total organic carbon.[98−100] To investigate the wettability alteration after the cyclic gas injection process, an air−liquid−rock system was used to determine the wettability of the shale cores before and after the cyclic tests. The cores were not cleaned by a solvent because the solvent can wash away the asphaltene particles and impact the results. Figure 17 shows equilibrated droplets of brine and the contact angles (i.e., right and left contact angle) of the cores with no pressure applied on them and cores after N_2 cyclic tests. To evaluate asphaltene deposition and the effect of gas injection on pore plugging on Eagle Ford cores, four separate saturated cores (Figure 17b) were used to measure the contact angle to which no pressure was applied (i.e., cores 9, 10, 11, and 12). These four cores are fully saturated with crude oil and the average of contact angle measured was 82.95°. This indicates that weakly intermediate wettability existed before applying the gas pressure. For accuracy purpose, the contact angles from all of the shale cores (Table 8) were determined after N_2 cyclic tests in both conditions (i.e., miscible and immiscible). The average contact angle following N_2 cycle testing was around 102.26°, showing that N_2 changed the wettability to a strong intermediate-wet system. These results suggest that N_2 influenced the deposition of asphaltene in the shale cores. The contact angle rose when miscible gas was injected, indicating that miscibility may generate a strongly intermediate-wet and close to oil-wet system during miscible N_2 cyclic gas injection. Our findings were quite similar with various experimental literature data, where the contact angle increased as the gas injection pressure increased.[101−105] This can be due to the fact that the shale surface structure had been altered by asphaltene deposition, making it rougher, resulting in an increase in contact angle readings.[106,107] Furthermore, our findings indicate that oil reduction and asphaltene deposition occurred in the later cycles since the decrease in oil recovery was detected in the last two cycles in the majority of the cyclic experiments discussed earlier. As more cycles were applied, asphaltene particles started to fill the big pores first at a higher rate[93] and more asphaltene was deposited in the cores along with an increase in the blockage rate, especially when using miscible N_2, which has a strong extraction of the hydrocarbon components. A reduction in the oil recovery factor followed the N_2 cyclic injections, and the influence of asphaltene deposition and precipitation on oil recovery was observed in subsequent cycles.[108] The results confirmed that cyclic gas injection, particularly at miscible pressures, affects the stability of the asphaltene clusters and reduced the strong

https://doi.org/10.1021/acs.energyfuels.2c02533
Energy Fuels 2022, 36, 12677−12694

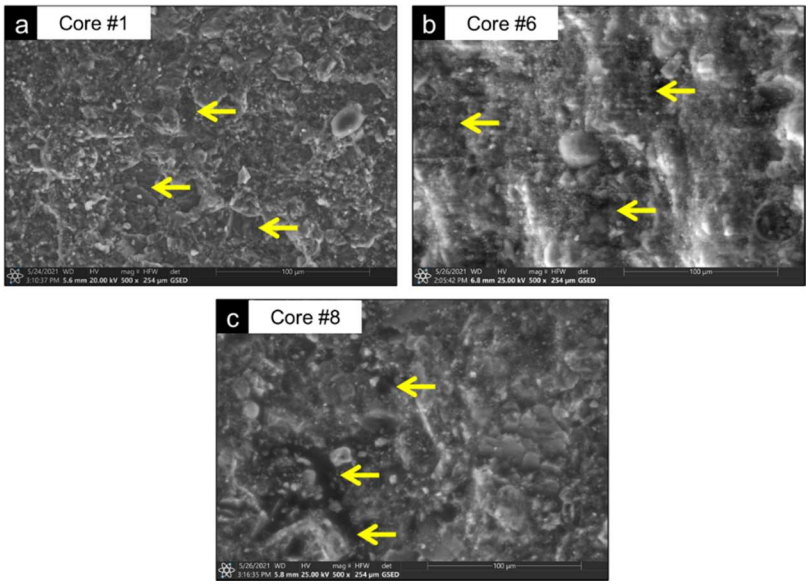

Figure 18. Scanning electron microscopy (SEM) images (100 μm) of three cores after cyclic N_2 gas injection tests.

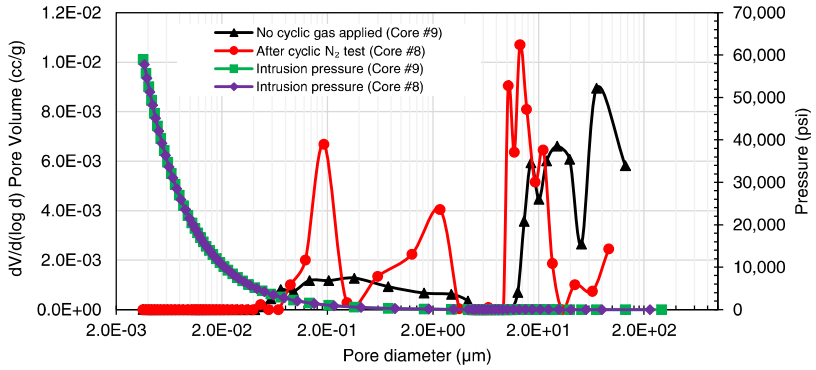

Figure 19. Pore size distribution of the tested cores before and after the N_2 cyclic gas injection mercury intrusion process.

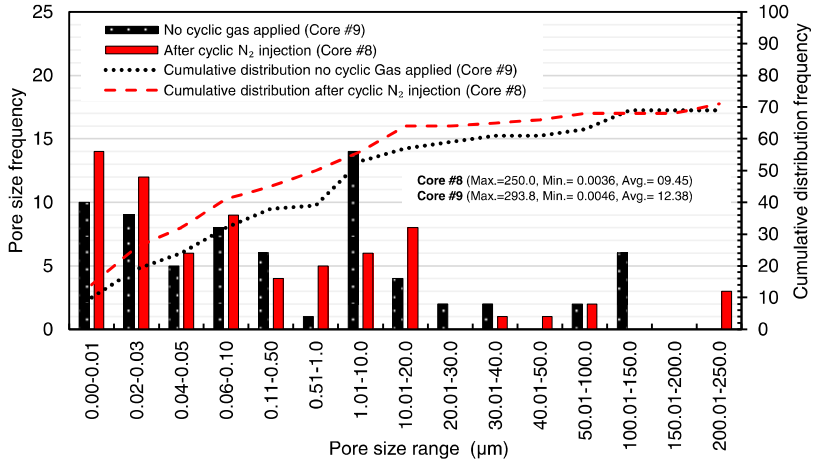

Figure 20. Comparison of the pore size distribution in Eagle Ford cores before and after the N_2 cyclic gas injection tests.

bonds between the asphaltene particles and resins, resulting in increased asphaltene deposition and precipitation, specifically in later cycles.

3.3.4. Scanning Electron Microscopy (SEM) Analysis. The primary goal of using the SEM was to reveal the impact of the asphaltene precipitation and deposition process in the shale formation after the cyclic tests. As presented in Figure 18, asphaltene deposition and pore plugging of shale cores were also investigated using a scanning electron microscope (SEM) at a magnification of 100 μm. SEM examination can help to show the asphaltene deposition inside the cores and give a more detailed study of the small pores of shale formation. Gas injection can disrupt the connections between the resins and asphaltene particles in crude oil, causing asphaltene deposition

https://doi.org/10.1021/acs.energyfuels.2c02533
Energy Fuels 2022, 36, 12677−12694

to increase. Asphaltene clusters may form in reservoir pores as a result of this mechanism. In this investigation, three samples were used for SEM examination following N_2 cyclic testing. Based on the SEM analysis, asphaltene clusters filled certain areas in the shale cores. For example, samples (a) and (c) showed more asphaltene pore blockage than sample (b), perhaps because to the longer soaking times of 6 and 24 h, respectively. Because of the different conditions of the injected pressure and the diverse structures of the samples, the severity of asphaltene deposition was clearer in samples (a) and (c) compared to sample (b). These photos confirm that cyclic N_2 injection changed the pore size structure inside the cores, and this led to lowering the oil recovery.

3.3.5. Pore Size Distribution due to Asphaltene Deposition. The purpose of this section is to evaluate and see how the pore size distribution of the cores changed as a result of asphaltene deposition after N_2 cyclic tests. The mercury porosimeter technique is a practical method for determining the pore size distribution of rocks, and it is effective for comparing the findings of similar materials.[111,112] Two Eagle Ford cores were selected to measure the pore size distribution using a PoreMaster mercury porosimeter. One sample (i.e., core #9) was selected from the samples that only saturated with crude oil and no pressure was applied. The results from this sample were compared to the other core (i.e., core #8) after applying cyclic N_2 pressure. Small pieces of each sample were needed; hence, each core was smashed into small pieces before the measurements. During the test, a maximum pressure of 60,000 psi was applied to examine the small pores and the throat inside the cores. The volume of intruded mercury was calculated and recorded automatically by the PoreMaster at each intrusion pressure. A comparison of the pore size distribution of the Eagle Ford cores is shown in Figures 19 and 20. As a result of gas injection, the composition of the oil in all cores changes, resulting in the precipitation of asphaltene. The asphaltene aggregated and produced a solid phase that began to accumulate inside the cores and on the rock's surface, plugging the pores.[113,114] By comparing the pore size distributions, lager pore size diameters were determined for the sample with no pressure applied compared to the other core. The figure demonstrates that the two samples' pore size peaks were in different ranges, indicating that the predominant pore diameter in the two samples was different. For instance, the peak of the pore size distribution of the sample before cyclic test was between 0.03 and 40 μm, but ranged between 0.01 and 20 μm after N_2 cyclic test. The intrusion of mercury into the sample selected after cyclic N_2 test was at a higher rate into the smaller pores. These results reveal that the pore throat in the cores had been impacted by the asphaltene clusters and particles after the cyclic N_2 gas injection applied. Our findings are consistent with our previously explained results and explain why the oil recovery was reduced at later cycles and wettability changes after cyclic N_2 tests.

4. CONCLUSIONS

A comprehensive experimental study was conducted to investigate asphaltene deposition and precipitation under cyclic N_2 injections using Eagle Ford shale cores (dynamic mode) and ultrasmall mesh filter paper membranes (static mode). The effect of pressure, miscibility, and soaking time was evaluated. To provide a holistic assessment of the influence of asphaltene deposition in such gas injection techniques, wettability analysis and pore size distribution evaluation of the cores were undertaken. The results support the following conclusions.

a. During the cyclic filtration experiments (i.e., static mode), the results showed that the asphaltene weight percent increased when increasing the pressure, and miscible pressure had the highest rate of asphaltene weight percent. Also, the impact of N_2 injection on asphaltene instability was found mainly in the first four cycles. Due to the lower pore size structure, the 50 nm filter membranes had a higher asphaltene weight percentage.
b. After the cyclic filtration experiments, chromatography analysis of the produced oil revealed that N_2 injection produced more heavy hydrocarbon components after the final cycle, especially under miscible conditions. The miscibility of N_2 gas extracted more light hydrocarbon components from the crude oil than immiscible conditions.
c. Using Eagle Ford cores under cyclic N_2 gas injection (i.e., dynamic mode) showed an increase in the oil recovery when increasing the pressure, and more cycles resulted in more oil recovery, especially during the early cycles. During miscible conditions, these observations were substantially more effective.
d. In the dynamic mode, the soaking time modes results demonstrated that starting with a shorter soaking period improved oil recovery. Longer soaking periods affected the deposition of asphaltene inside the cores, increasing the speed drop in oil recovery. In all experiments, longer soaking time led to higher oil recovery.
e. Our findings imply that oil reduction and asphaltene deposition occurred in the later cycles because the majority of cyclic tests revealed a reduction in oil recovery in the last two cycles. The asphaltene particles began to fill the bigger pores at a faster rate as the number of cycles increased, converting the wettability of the shale cores to a strongly intermediate-wet system.
f. A smaller pore size distribution was determined using a PoreMaster mercury porosimeter of the cores after the cyclic experiments, indicating that the asphaltene particles reduced the size of the pores.

■ ASSOCIATED CONTENT

Supporting Information

The Supporting Information is available free of charge at https://pubs.acs.org/doi/10.1021/acs.energyfuels.2c02533.

Weight of all Eagle Ford cores before and after the saturation process (PDF)

■ AUTHOR INFORMATION

Corresponding Author

Abdulmohsin Imqam − *Missouri University of Science and Technology, Rolla, Missouri 65401, United States;* orcid.org/0000-0003-1783-7491; Phone: +1(573) 341-4669; Email: aimqam@mst.edu

Author

Mukhtar Elturki − *Missouri University of Science and Technology, Rolla, Missouri 65401, United States; Misurata University, Misrata 80045, Libya;* orcid.org/0000-0001-9331-0021

Complete contact information is available at:

https://doi.org/10.1021/acs.energyfuels.2c02533
Energy Fuels 2022, 36, 12677−12694

https://pubs.acs.org/10.1021/acs.energyfuels.2c02533

Funding

M.E.: methodology, conceptualization, experimentation, investigation, formal analysis, visualization, writing—original draft, and writing—review and editing. A.I.: conceptualization, validation, writing—review and editing, and supervision and funding.

Notes

The authors declare no competing financial interest.

■ ACKNOWLEDGMENTS

The authors acknowledge the National Science Foundation, Chemical, Biological, Environmental, and Transport systems for funding the work under grant no. CBET-1932965.

■ REFERENCES

(1) Elturki, M.; Imqam, A.*Application of Enhanced Oil Recovery Methods in Unconventional Reservoirs: A Review and Data Analysis*; American Rock Mechanics Association, 2020.
(2) Warpinski, N. R.; Mayerhofer, M. J.; Vincent, M. C.; Cipolla, C. L.; Lolon, E. P. Stimulating unconventional reservoirs: maximizing network growth while optimizing fracture conductivity. *J. Can. Pet. Technol.* **2009**, *48*, 39−51.
(3) Sheng, J. J. Enhanced oil recovery in shale reservoirs by gas injection. *J. Nat. Gas Sci. Eng.* **2015**, *22*, 252−259.
(4) Zoback, M. D.; Kohli, A. H.*Unconventional Reservoir Geomechanics*; Cambridge University Press, 2019.
(5) Ahmed, S.; Elldakli, F.; Heinze, L.; Elwegaa, K.; Emadi, E. Investigating Effects of the Ball Size on the Gas Throughput Using Partially Curved and Wholly Curved Seats. *Int. J. Pet. Petrochem. Eng.* **2019**, *5*, 1−9.
(6) Ahmed, S.; Emadi, H.; Heinze, L.; Elwegaa, K.; Elldakli, F. An experimental comparison between actual valve and benchmark valve using modified design and optimized design. *SSRG Int. J. Eng. Trends Technol.* **2020**, *68*, 64−73.
(7) Ahmed, S.Investigating Effects of the Ball Configuration on the Gas Throughput Using Partially Curved and Wholly Curved Seats. Doctoral Dissertation, Texas Tech University, 2020.
(8) Ge, X.; Biheri, G.; Imqam, A. In *Comparative Study of Anionic and Cationic High Viscosity Friction Reducers in High-TDS Marcellus Shale Formation Water*, Paper presented at the 56th U.S. Rock Mechanics/Geomechanics Symposium, Santa Fe, New Mexico, 2022.
(9) Liu, J.; Sheng, J. J.; Emadibaladehi, H.; Tu, J. Experimental study of the stimulating mechanism of shut-in after hydraulic fracturing in unconventional oil reservoirs. *Fuel* **2021**, *300*, No. 120982.
(10) Elturki, M.; McElroy, P. D.; Li, D.; Kablan, A.; Shaglouf, H. In *Simulation Study Investigating the Impact of Carbon Dioxide Foam Fracturing Fluids on Proppant Transport*, SPE Trinidad and Tobago Section Energy Resources Conference, OnePetro, 2021.
(11) Biheri, G.; Imqam, A. In *Proppant Transport by High Viscosity Friction Reducer and Guar Linear Gel-Based Fracture Fluids*, 54th US Rock Mechanics/Geomechanics Symposium, OnePetro, 2020.
(12) Biheri, G.; Imqam, A. Settling of Spherical Particles in High Viscosity Friction Reducer Fracture Fluids. *Energies* **2021**, *14*, 2462.
(13) Biheri, G.; Imqam, A. Proppant Transport Using High-Viscosity Friction Reducer Fracture Fluids at High-Temperature Environment. *SPE J.* **2021**, 1−17.
(14) Biheri, G.; Imqam, A. In *Experimental Study: High Viscosity Friction Reducer Fracture Fluid Rheological Advantages Over the Guar Linear Gel*, 55th US Rock Mechanics/Geomechanics Symposium, OnePetro, 2021.
(15) Biheri, G.; Imqam, A. In *Experimental Study: Determine the Impact of Temperature on Proppant Settling Velocity Utilizing HVFR and Linear Guar*, Paper presented at the 56th U.S. Rock Mechanics/Geomechanics Symposium, Santa Fe, New Mexico, 2022.
(16) Biheri, G.; Elmaleh, K.; Imqam, A. In *Experimental Study: Investigate the Proppant Settling Velocity in Static and Dynamic Model Using High Viscosity Friction Reducer and Linear Guar*, Paper Presented at the 56th U.S. Rock Mechanics/Geomechanics Symposium, Santa Fe, New Mexico, 2022.
(17) Biheri, G.; Elmaleh, K.; Amoura, A.; Imqam, A. In *The Impact of high TDS of Utica Shale on High Viscosity Friction Reducer Performance: Experimental Study*, Paper presented at the SPE Eastern Regional Meeting, Wheeling, West Virginia, USA, 2022.
(18) Ge, X.; Biheri, G.; Imqam, A. In *Proppant Transport Analysis of The Anionic High Viscosity Friction Reducer in High-TDS Marcellus Shale Formation Water Environments*, Paper presented at the SPE Eastern Regional Meeting, Wheeling, West Virginia, USA, 2022.
(19) Biheri, G.; Amoura, A.; Elmaleh, K.; Nouh, A. In *A Field Study: Minimizing Gas Flaring Through Reuse to Produce Electricity and Petrochemical Products*, Paper presented at the SPE Eastern Regional Meeting, Wheeling, West Virginia, USA, 2022.
(20) Yang, P.; Guo, H.; Yang, D. Determination of residual oil distribution during waterflooding in tight oil formations with NMR relaxometry measurements. *Energy Fuels* **2013**, *27*, 5750−5756.
(21) Ahmad, H. M.; Kamal, M. S.; Mahmoud, M.; Shakil Hussain, S. M.; Abouelresh, M.; Al-Harthi, M. A. Organophilic clay-based drilling fluids for mitigation of unconventional shale reservoirs instability and formation damage. *J. Energy Resour. Technol.* **2019**, *141*, No. 093102.
(22) Milad, M.; Junin, R.; Sidek, A.; Imqam, A.; Tarhuni, M. Huff-n-Puff Technology for Enhanced Oil Recovery in Shale/Tight Oil Reservoirs: Progress, Gaps, and Perspectives. *Energy Fuels* **2021**, *35*, 17279−17333.
(23) Tang, W.; Sheng, J. J. Huff-n-puff gas injection or gas flooding in tight oil reservoirs? *J. Pet. Sci. Eng.* **2022**, *208*, No. 109725.
(24) Jia, B.; Tsau, J. S.; Barati, R. A review of the current progress of CO2 injection EOR and carbon storage in shale oil reservoirs. *Fuel* **2019**, *236*, 404−427.
(25) Shi, B.; Song, S.; Chen, Y.; et al. Status of Natural Gas Hydrate Flow Assurance Research in China: A Review. *Energy Fuels* **2021**, *35*, 3611−3658.
(26) Hassanpouryouzband, A.; Joonaki, E.; Vasheghani Farahani, M.; et al. Gas hydrates in sustainable chemistry. *Chem. Soc. Rev.* **2020**, *49*, 5225−5309.
(27) Ali, S. I.; Lalji, S. M.; Haneef, J.; Ahsan, U.; Tariq, S. M.; Tirmizi, S. T.; Shamim, R. Critical analysis of different techniques used to screen asphaltene stability in crude oils. *Fuel* **2021**, *299*, No. 120874.
(28) Fakher, S.; Ahdaya, M.; Elturki, M.; Imqam, A. Critical review of asphaltene properties and factors impacting its stability in crude oil. *J. Pet. Explor. Prod. Technol.* **2020**, *10*, 1183−1200.
(29) Zhou, X.; Yuan, Q.; Peng, X.; Zeng, F.; Zhang, L. A critical review of the CO2 huff 'n'puff process for enhanced heavy oil recovery. *Fuel* **2018**, *215*, 813−824.
(30) Elturki, M.; Imqam, A. In *High Pressure-High Temperature Nitrogen Interaction with Crude Oil and Its Impact on Asphaltene Deposition in Nano Shale Pore Structure: An Experimental Study*, SPE/AAPG/SEG Unconventional Resources Technology Conference, OnePetro, 2020.
(31) Jafari Behbahani, T.; Ghotbi, C.; Taghikhani, V.; Shahrabadi, A. A modified scaling equation based on properties of bottom hole live oil for asphaltene precipitation estimation under pressure depletion and gas injection conditions. *Fluid Phase Equilib.* **2013**, *358*, 212−219.
(32) Turta, A. T.; Najman, J.; Singhal, A. K.; Leggitt, S.; Fisher, D. In *Permeability Impairment due to Asphaltenes during Gas Miscible Flooding and its Mitigation*, International Symposium on Oilfield Chemistry, Society of Petroleum Engineers, 1997.
(33) Sim, S. S. K.; Okatsu, K.; Takabayashi, K.; Fisher, D. B.*Asphaltene-Induced Formation Damage: Effect of Asphaltene Particle Size and Core Permeability*, SPE Annual Technical Conference and Exhibition, Society of Petroleum Engineers, 2005.
(34) Hamadou, R.; Khodja, M.; Kartout, M.; Jada, A. Permeability reduction by asphaltenes and resins deposition in porous media. *Fuel* **2008**, *87*, 2178−2185.

(35) Jafari Behbahani, T.; Ghotbi, C.; Taghikhani, V.; Shahrabadi, A. Investigation of asphaltene adsorption in sandstone core sample during CO2 injection: Experimental and modified modeling. *Fuel* **2014**, *133*, 63−72.
(36) Mehana, M.; Abraham, J.; Fahes, M. The impact of asphaltene deposition on fluid flow in sandstone. *J. Pet. Sci. Eng.* **2019**, *174*, 676−681.
(37) Lo, P. A.; Tinni, A. O.; Milad, B. Experimental study on the influences of pressure and flow rates in the deposition of asphaltenes in a sandstone core sample. *Fuel* **2022**, *310*, No. 122420.
(38) Fakher, S.; Imqam, A. Asphaltene precipitation and deposition during CO2 injection in nano shale pore structure and its impact on oil recovery. *Fuel* **2019**, *237*, 1029−1039.
(39) Afra, S.; Samouei, H.; Golshahi, N.; Nasr-El-Din, H. Alterations of asphaltenes chemical structure due to carbon dioxide injection. *Fuel* **2020**, *272*, No. 117708.
(40) Elturki, M.; Imqam, A. In *An Experimental Investigation of Asphaltene Aggregation Under Carbon Dioxide Injection Flow in Ultra-Low-Permeability Pore Structure*, SPE Canadian Energy Technology Conference, OnePetro, 2022.
(41) Elturki, M.; Imqam, A. Asphaltene Precipitation and Deposition under Miscible and Immiscible Carbon Dioxide Gas Injection in Nanoshale Pore Structure. *SPE J.* **2022**, 1−17.
(42) Espinoza Mejia, J. E.; Li, X.; Zheng, R. In *Experimental Study of Asphaltene Precipitation and Deposition During Immiscible CO2-EOR Process*, SPE International Conference and Exhibition on Formation Damage Control, OnePetro, 2022.
(43) Wang, P.; Zhao, F.; Hou, J.; Lu, G.; Zhang, M.; Wang, Z. Comparative analysis of CO2, N2, and gas mixture injection on asphaltene deposition pressure in reservoir conditions. *Energies* **2018**, *11*, 2483.
(44) Jamaluddin, A. K. M.; Joshi, N.; Iwere, F.; Gurpinar, O. In *An Investigation of Asphaltene Instability Under Nitrogen Injection*, SPE International Petroleum Conference and Exhibition in Mexico, Society of Petroleum Engineers, 2002.
(45) Zadeh, G. A.; Moradi, S.; Dabir, B.; Emadi, M. A.; Rashtchian, D. In *Comprehensive Study of Asphaltene Precipitation due to Gas Injection: Experimental Investigation and Modeling*, SPE Enhanced Oil Recovery Conference, OnePetro, 2011.
(46) Moradi, S.; Dabir, B.; Rashtchian, D.; Mahmoudi, B. Effect of miscible nitrogen injection on instability, particle size distribution, and fractal structure of asphaltene aggregates. *J. Dispersion Sci. Technol.* **2012**, *33*, 763−770.
(47) Khalaf, M. H.; Mansoori, G. A. Asphaltenes aggregation during petroleum reservoir air and nitrogen flooding. *J. Pet. Sci. Eng.* **2019**, *173*, 1121−1129.
(48) Elturki, M.; Imqam, A. In *An Experimental Study Investigating the Impact of Miscible and Immiscible Nitrogen Injection on Asphaltene Instability in Nano Shale Pore Structure*, SPE International Conference on Oilfield Chemistry, OnePetro, 2021.
(49) Elturki, M.; Imqam, A. Asphaltene Thermodynamic Flocculation during Immiscible Nitrogen Gas Injection. *SPE J.* **2021**, *26*, 3188−3204.
(50) Abedini, A.; Torabi, F. Oil recovery performance of immiscible and miscible CO2 huff-and-puff processes. *Energy Fuels* **2014**, *28*, 774−784.
(51) Yu, W.; Lashgari, H. R.; Wu, K.; Sepehrnoori, K. CO2 injection for enhanced oil recovery in Bakken tight oil reservoirs. *Fuel* **2015**, *159*, 354−363.
(52) Li, L.; Su, Y.; Sheng, J. J.; et al. Experimental and numerical study on CO2 sweep volume during CO2 huff-n-puff enhanced oil recovery process in shale oil reservoirs. *Energy Fuels* **2019**, *33*, 4017−4032.
(53) Elwegaa, K.; Emadi, H.; Soliman, M.; Gamadi, T.; Elsharafi, M. Improving oil recovery from shale oil reservoirs using cyclic cold carbon dioxide injection−An experimental study. *Fuel* **2019**, *254*, No. 115586.
(54) Zhu, Z.; Fang, C.; Qiao, R.; Yin, X.; Ozkan, E. Experimental and Molecular Insights on Mitigation of Hydrocarbon Sieving in Niobrara Shale by CO2 Huff 'N'Puff. *SPE J.* **2020**, *25*, 1803−1811.
(55) Fakher, S.; Imqam, A. Application of carbon dioxide injection in shale oil reservoirs for increasing oil recovery and carbon dioxide storage. *Fuel* **2020**, *265*, No. 116944.
(56) Badrouchi, N.; Pu, H.; Smith, S.; Badrouchi, F. Evaluation of CO2 enhanced oil recovery in unconventional reservoirs: Experimental parametric study in the Bakken. *Fuel* **2022**, *312*, No. 122941.
(57) Louk, K.; Ripepi, N.; Luxbacher, K.; et al. Monitoring CO2 storage and enhanced gas recovery in unconventional shale reservoirs: Results from the Morgan County, Tennessee injection test. *J. Nat. Gas Sci. Eng.* **2017**, *45*, 11−25.
(58) Sheng, J. J.; Chen, K. Evaluation of the EOR potential of gas and water injection in shale oil reservoirs. *J. Unconv. Oil Gas Resour.* **2014**, *5*, 1−9.
(59) Sanchez-Rivera, D.; Mohanty, K.; Balhoff, M. Reservoir simulation and optimization of Huff-and-Puff operations in the Bakken Shale. *Fuel* **2015**, *147*, 82−94.
(60) Sun, J.; Zou, A.; Sotelo, E.; Schechter, D. Numerical simulation of CO2 huff-n-puff in complex fracture networks of unconventional liquid reservoirs. *J. Nat. Gas Sci. Eng.* **2016**, *31*, 481−492.
(61) Wang, L.; Yu, W. Mechanistic simulation study of gas Puff and Huff process for Bakken tight oil fractured reservoir. *Fuel* **2019**, *239*, 1179−1193.
(62) Luo, Y.; Zheng, T.; Xiao, H.; Liu, X.; Zhang, H.; Wu, Z.; Zhao, X.; Xia, D. Identification of distinctions of immiscible CO2 huff and puff performance in Chang-7 tight sandstone oil reservoir by applying NMR, microscope and reservoir simulation. *J. Pet. Sci. Eng.* **2022**, *209*, No. 109719.
(63) Altawati, F.; Emadi, H.; Khalil, R.; Heinze, L.; Menouar, H. An experimental investigation of improving Wolfcamp Shale-Oil recovery using Liquid-N2-assisted N2 and/or CO2 Huff-n-Puff injection technique. *Fuel* **2022**, *324*, No. 124450.
(64) Wan, T.; Zhang, J.; Jing, Z. Experimental evaluation of enhanced shale oil recovery in pore scale by CO2 in Jimusar reservoir. *J. Pet. Sci. Eng.* **2022**, *208*, No. 109730.
(65) Zheng, T.; Yang, Z.; Liu, X.; Luo, Y.; Xiao, Q.; Zhang, Y.; Zhao, X. Understanding Immiscible Natural Gas Huff-N-Puff Seepage Mechanism in Porous Media: A Case Study of CH 4 Huff-N-Puff by Laboratory Numerical Simulations in Chang-7 Tight Core. *Nat. Resour. Res.* **2021**, *30*, 2397−2411.
(66) Baek, S.; Akkutlu, I. Y. Enhanced Recovery of Nanoconfined Oil in Tight Rocks Using Lean Gas (C2H6 and CO2) Injection. *SPE J.* **2021**, *26*, 1−20.
(67) Mahzari, P.; Mitchell, T. M.; Jones, A. P.; et al. Novel laboratory investigation of huff-n-puff gas injection for shale oils under realistic reservoir conditions. *Fuel* **2021**, *284*, No. 118950.
(68) Sie, C. Y.; Nguyen, Q. P. Field gas huff-n-puff for enhancing oil recovery in Eagle Ford shales−Effect of reservoir rock and crude properties. *Fuel* **2022**, *328*, No. 125127.
(69) Shilov, E.; Dorhjie, D. B.; Mukhina, E.; Zvada, M.; Kasyanenko, A.; Cheremisin, A. Experimental and numerical studies of rich gas Huff-n-Puff injection in tight formation. *J. Pet. Sci. Eng.* **2022**, *208*, No. 109420.
(70) Yu, Y.; Sheng, J. J. In *An Experimental Investigation of the Effect of Pressure Depletion Rate on Oil Recovery from Shale Cores by Cyclic N2 Injection*, Unconventional Resources Technology Conference, OnePetro, 2015.
(71) Altawati, F. S.An Experimental Study of the Effect of Water Saturation on Cyclic N2 and CO2 Injection in Shale Oil Reservoir. Doctoral Dissertation, Texas Tech University, 2016.
(72) Yu, Y.; Li, L.; Sheng, J. J. A comparative experimental study of gas injection in shale plugs by flooding and huff-n-puff processes. *J. Nat. Gas Sci. Eng.* **2017**, *38*, 195−202.
(73) Elwegaa, K.; Emadi, H. Improving oil recovery from shale oil reservoirs using cyclic cold nitrogen injection−An experimental study. *Fuel* **2019**, *254*, No. 115716.

https://doi.org/10.1021/acs.energyfuels.2c02533
Energy Fuels 2022, 36, 12677−12694

(74) Xiong, X.; Sheng, J. J.; Wu, X.; Qin, J. Experimental investigation of foam-assisted N2 huff-n-puff enhanced oil recovery in fractured shale cores. *Fuel* **2022**, *311*, No. 122597.
(75) Li, L.; Zhang, Y.; Sheng, J. J. Effect of the injection pressure on enhancing oil recovery in shale cores during the CO2 huff-n-puff process when it is above and below the minimum miscibility pressure. *Energy Fuels* **2017**, *31*, 3856−3867.
(76) Tovar, F. D.; Barrufet, M. A.; Schechter, D. S. Enhanced Oil Recovery in the Wolfcamp Shale by Carbon Dioxide or Nitrogen Injection: An Experimental Investigation. *SPE J.* **2021**, *26*, 515−537.
(77) Bougre, E. S.; Gamadi, T. D. Enhanced oil recovery application in low permeability formations by the injections of CO2, N2 and CO2/N2 mixture gases. *J. Pet. Explor. Prod. Technol.* **2021**, *11*, 1963−1971.
(78) Shen, Z.; Sheng, J. J. Experimental study of permeability reduction and pore size distribution change due to asphaltene deposition during CO2 huff and puff injection in Eagle Ford shale. *Asia-Pac. J. Chem. Eng.* **2017**, *12*, 381−390.
(79) Shen, Z.; Sheng, J. J. Investigation of asphaltene deposition mechanisms during CO2 huff-n-puff injection in Eagle Ford shale. *Pet. Sci. Technol.* **2017**, *35*, 1960−1966.
(80) Mohammad, R. S.; Zhang, S.; Lu, S.; Jamal-Ud-Din, S.; Zhao, X. Simulation study of asphaltene deposition and solubility of CO2 in the brine during cyclic CO2 injection process in unconventional tight reservoirs. *Int. J. Geol. Environ. Eng.* **2017**, *11*, 495−5.
(81) Lee, J. H.; Lee, K. S. Investigation of asphaltene-derived formation damage and nano-confinement on the performance of CO2 huff-n-puff in shale oil reservoirs. *J. Pet. Sci. Eng.* **2019**, *182*, No. 106304.
(82) Shen, Z.; Sheng, J. J. Optimization Strategy to Reduce Asphaltene Deposition-Associated Damage During CO 2 Huff-n-Puff Injection in Shale. *Arabian J. Sci. Eng.* **2019**, *44*, 6179−6193.
(83) Li, L.; Su, Y.; Lv, Y.; Tu, J. Asphaltene deposition and permeability impairment in shale reservoirs during CO2 huff-n-puff EOR process. *Pet. Sci. Technol.* **2020**, *38*, 384−390.
(84) Elturki, M.; Imqam, A. Asphaltene Thermodynamic Precipitation during Miscible Nitrogen Gas Injection. *SPE J.* **2022**, *27*, 877−894.
(85) Elturki, M.; Imqam, A. In *Analysis of Nitrogen Minimum Miscibility Pressure MMP and Its Impact on Instability of Asphaltene Aggregates-An Experimental Study*, SPE Trinidad and Tobago Section Energy Resources Conference, OnePetro, 2021.
(86) Sebastian, H. M.; Lawrence, D. D. In *Nitrogen Minimum Miscibility Pressures*, SPE/DOE Enhanced Oil Recovery Symposium, Society of Petroleum Engineers, 1992.
(87) Vahidi, A.; Zargar, G. In *Sensitivity Analysis of Important Parameters Affecting Minimum Miscibility Pressure (MMP) of Nitrogen Injection into Conventional Oil Reservoirs*, SPE/EAGE Reservoir Characterization and Simulation Conference, Society of Petroleum Engineers, 2007.
(88) Belhaj, H.; Abu Khalifeh, H. A.; Javid, K. In*Potential of Nitrogen Gas Miscible Injection in South East Assets, Abu Dhabi*, North Africa Technical Conference and Exhibition, Society of Petroleum Engineers, 2013.
(89) Zolghadr, A.; Riazi, M.; Escrochi, M.; Ayatollahi, S. Investigating the effects of temperature, pressure, and paraffin groups on the N2 miscibility in hydrocarbon liquids using the interfacial tension measurement method. *Ind. Eng. Chem. Res.* **2013**, *52*, 9851−9857.
(90) Barati-Harooni, A.; Najafi-Marghmaleki, A.; Hoseinpour, S. A.; Tatar, A.; Karkevandi-Talkhooncheh, A.; Hemmati-Sarapardeh, A.; Mohammadi, A. H. Estimation of minimum miscibility pressure (MMP) in enhanced oil recovery (EOR) process by N2 flooding using different computational schemes. *Fuel* **2019**, *235*, 1455−1474.
(91) Chung, T. H. In *Thermodynamic Modeling for Organic Solid Precipitation*, SPE Annual Technical Conference and Exhibition, Society of Petroleum Engineers, 1992.
(92) Fu, Q.; Cudjoe, S.; Barati Ghahfarokhi, R.; et al. Investigating the role of diffusion in hydrocarbon gas huff-n-puff injection-an Eagle Ford study. *J. Pet. Sci. Eng.* **2021**, *198*, No. 108146.
(93) Huang, X.; Zhang, Y.; He, M.; Li, X.; Yang, W.; Lu, J. Asphaltene precipitation and reservoir damage characteristics of CO2 flooding in different microscopic structure types in tight light oil reservoirs. *Fuel* **2022**, *312*, No. 122943.
(94) Abdallah, W.; et al. Fundamentals of wettability. *Technology* **1986**, *38*, 268.
(95) Sheng, J. J. Discussion of shale rock wettability and the methods to determine it. *Asia-Pac. J. Chem. Eng.* **2018**, *13*, No. e2263.
(96) Odusina, E.; Sondergeld, C.; Rai, C. In *An NMR Study on Shale Wettability*, Canadian Unconventional Resources Conference, OnePetro, 2011.
(97) Akbarabadi, M.; Saraji, S.; Piri, M.; Georgi, D.; Delshad, M. Nano-scale experimental investigation of in-situ wettability and spontaneous imbibition in ultra-tight reservoir rocks. *Adv. Water Resour.* **2017**, *107*, 160−179.
(98) Kumar, K.; Dao, E. K.; Mohanty, K. K. Atomic force microscopy study of wettability alteration by surfactants. *SPE J.* **2008**, *13*, 137−145.
(99) Pan, B.; Li, Y.; Zhang, M.; Wang, X.; Iglauer, S. Effect of total organic carbon (TOC) content on shale wettability at high pressure and high temperature conditions. *J. Pet. Sci. Eng.* **2020**, *193*, No. 107374.
(100) Mohammed, I.; Mahmoud, M.; El-Husseiny, A.; Al Shehri, D.; Al-Garadi, K.; Kamal, M. S.; Alade, O. S. Impact of Asphaltene Precipitation and Deposition on Wettability and Permeability. *ACS Omega* **2021**, *6*, 20091−20102.
(101) Sarmadivaleh, M.; Al-Yaseri, A. Z.; Iglauer, S. Influence of temperature and pressure on quartz−water−CO2 contact angle and CO2−water interfacial tension. *J. Colloid Interface Sci.* **2015**, *441*, 59−64.
(102) Iglauer, S.; Al-Yaseri, A. Z.; Rezaee, R.; Lebedev, M. CO2 wettability of caprocks: Implications for structural storage capacity and containment security. *Geophys. Res. Lett.* **2015**, *42*, 9279−9284.
(103) Arif, M.; Al-Yaseri, A. Z.; Barifcani, A.; Lebedev, M.; Iglauer, S. Impact of pressure and temperature on CO2−brine−mica contact angles and CO2−brine interfacial tension: Implications for carbon geo-sequestration. *J. Colloid Interface Sci.* **2016**, *462*, 208−215.
(104) Roshan, H.; Al-Yaseri, A. Z.; Sarmadivaleh, M.; Iglauer, S. On wettability of shale rocks. *J. Colloid Interface Sci.* **2016**, *475*, 104−111.
(105) Pan, B.; Li, Y.; Wang, H.; Jones, F.; Iglauer, S. CO2 and CH4 wettabilities of organic-rich shale. *Energy Fuels* **2018**, *32*, 1914−1922.
(106) Sayyad Amin, J.; Nikooee, E.; Ayatollahi, S.; Alamdari, A. Investigating wettability alteration due to asphaltene precipitation: Imprints in surface multifractal characteristics. *Appl. Surf. Sci.* **2010**, *256*, 6466−6472.
(107) Hosseini, E. Experimental investigation of effect of asphaltene deposition on oil relative permeability, rock wettability alteration, and recovery in WAG process. *Pet. Sci. Technol.* **2019**, *37*, 2150−2159.
(108) Shen, Z.; Sheng, J. J. Experimental and numerical study of permeability reduction caused by asphaltene precipitation and deposition during CO2 huff and puff injection in Eagle Ford shale. *Fuel* **2018**, *211*, 432−445.
(109) Anderson, W. Wettability literature survey-part 2: Wettability measurement. *J. Pet. Technol.* **1986**, *38*, 1246−1262.
(110) Arif, M.; Lebedev, M.; Barifcani, A.; Iglauer, S. Influence of shale-total organic content on CO2 geo-storage potential. *Geophys. Res. Lett.* **2017**, *44*, 8769−8775.
(111) Giesche, H. Mercury porosimetry: a general (practical) overview. *Part. Part. Syst. Charact.* **2006**, *23*, 9−19.
(112) Labani, M. M.; Rezaee, R.; Saeedi, A.; Al Hinai, A. Evaluation of pore size spectrum of gas shale reservoirs using low pressure nitrogen adsorption, gas expansion and mercury porosimetry: A case study from the Perth and Canning Basins, Western Australia. *J. Pet. Sci. Eng.* **2013**, *112*, 7−16.
(113) Jafari Behbahani, T.; Ghotbi, C.; Taghikhani, V.; Shahrabadi, A. Experimental study and mathematical modeling of asphaltene

https://doi.org/10.1021/acs.energyfuels.2c02533
Energy Fuels 2022, 36, 12677−12694

deposition mechanism in core samples. *Oil Gas Sci. Technol.* **2015**, *70*, 1051−1074.
(114) Shen, Z.; Sheng, J. J. In *Experimental Study of Asphaltene Aggregation during CO2 and CH4 Injection in Shale Oil Reservoirs*, SPE Improved Oil Recovery Conference, OnePetro, 2016.

Recommended by ACS

A Comparison between the Perturbed-Chain Statistical Associating Fluid Theory Equation of State and Machine Learning Modeling Approaches in Asphaltene Onset Pres...

Simin Tazikeh, Oleksandr P. Ivakhnenko, *et al.*
AUGUST 16, 2022
ACS OMEGA
READ

Macro- and Microanalysis on Noncondensable Gas Antiwater Invasion in a Bottom Water Reservoir with a Rupturable Interlayer

Zhanxi Pang, Yuhao Zhou, *et al.*
OCTOBER 11, 2022
ACS OMEGA
READ

Influence of Well Types on Optimizing the Co-production of Gas from Coal and Tight Formations

Guanglei Cui, Zhejun Pan, *et al.*
JUNE 09, 2022
ENERGY & FUELS
READ

Diffusion Mechanisms of Dissolved Gases in Transformer Oil Influenced with Moisture Based on Molecular Dynamics Simulation

Tianyan Jiang, Xin Zhou, *et al.*
OCTOBER 26, 2022
ACS OMEGA
READ

Get More Suggestions >

https://doi.org/10.1021/acs.energyfuels.2c02533
Energy Fuels 2022, 36, 12677−12694